The Greenhouse Gas Climate Change Initiative (GHG-CCI): Comparison and quality assessment of near-surface-sensitive satellite-derived CO2 and CH4 global data sets

M. Buchwitz, M. Reuter, O. Schneising, H. Boesch, S. Guerlet, B. Dils, I. Aben, Raymond Armante, P. Bergamaschi, T. Blumenstock, et al.

The Greenhouse Gas Climate Change Initiative (GHG-CCI): comparison and quality assessment of near-surface-sensitive satellite-derived CO_2 and CH_4 global data sets

M. Buchwitz,[1,], M. Reuter[1], O. Schneising[1], H. Boesch[2], S. Guerlet,[3,#], B. Dils[4], I. Aben[3], R. Armante[6], P. Bergamaschi[10], T. Blumenstock[7], H. Bovensmann[1], D. Brunner[8], B. Buchmann[8], J. P. Burrows[1], A. Butz[7], A. Chédin[6], F. Chevallier[9], C. D. Crevoisier[6], N. M. Deutscher[1, 16], C. Frankenberg[11,20], F. Hase[7], O. P. Hasekamp[3], J. Heymann[1], T. Kaminski[12], A. Laeng[7], G. Lichtenberg[5], M. De Mazière[4], S. Noël[1], J. Notholt[1], J. Orphal[7], C. Popp[8, §], R. Parker[2], M. Scholze[12,13], R. Sussmann[7], G. P. Stiller[7], T. Warneke[1], C. Zehner[14], A. Bril[15], D. Crisp[11], D. W. T. Griffith[16], A. Kuze[17], C. O'Dell[18], S. Oshchepkov[15], V. Sherlock[19], H. Suto[17], P. Wennberg[20], D. Wunch[20], T. Yokota[15], Y. Yoshida[15]*

1. Institute of Environmental Physics (IUP), University of Bremen, Bremen, Germany

2. University of Leicester, Leicester, United Kingdom.

3. SRON Netherlands Institute for Space Research, Utrecht, Netherlands.

4. Belgian Institute for Space Aeronomy (BIRA), Brussels, Belgium.

5. Deutsches Zentrum für Luft- und Raumfahrt (DLR), Oberpfaffenhofen, Germany.

6. Laboratoire de Météorologie Dynamique (LMD), Palaiseau, France.

7. Karlsruhe Institute of Technology (KIT), Karlsruhe and Garmisch-Partenkirchen, Germany.

8. Swiss Federal Laboratories for Materials Science and Technology (Empa), Dübendorf, Switzerland.

9. Laboratoire des Sciences du Climate et de l'Environment (LSCE), Gif-sur-Yvette, France.

10. European Commission Joint Research Centre (EC-JRC), Institute for Environment and Sustainability (IES), Air and Climate Unit, Ispra, Italy.

11. Jet Propulsion Laboratory (JPL), Pasadena, California, United States of America.

12. FastOpt GmbH, Hamburg, Germany.

13. University of Bristol, Bristol, United Kingdom.

14. European Space Agency (ESA), ESRIN, Frascati, Italy.

15. National Institute for Environmental Studies (NIES), Tsukuba, Japan.

16. University of Wollongong, Wollongong, Australia.

17. Japan Aerospace Exploration Agency (JAXA), Tsukuba, Japan.

18.Colorado State University (CSU), Fort Collins, Colorado, United States of America.

19. National Institute of Water and Atmospheric Research (NIWA), Lauder, New Zealand.

20. California Institute of Technology, Pasadena, California, United States of America.

#) Now at: Laboratoire de Météorologie Dynamique (LMD), Institut Pierre-Simon Laplace, Paris, France.

§) Now at: National Museum of Natural History, Smithsonian Institution, Washington, DC, USA, and Harvard-Smithsonian Center for Astrophysics, Cambridge, Massachusetts, USA.

**) Corresponding author: Michael Buchwitz, Institute of Environmental Physics (IUP), University of Bremen, FB1, Otto Hahn Allee 1, 28334 Bremen, Germany, Phone: +49-(0)421-218-62086, Fax: +49-(0)421-218-62070, E-mail: Michael.Buchwitz@iup.physik.uni-bremen.de.*

Abstract

The GHG-CCI project is one of several projects of the European Space Agency's (ESA) Climate Change Initiative (CCI). The goal of the CCI is to generate and deliver data sets of various satellite-derived Essential Climate Variables (ECVs) in line with GCOS (Global Climate Observing System) requirements. The "ECV Greenhouse Gases" (ECV GHG) is the global distribution of important climate relevant gases – atmospheric CO_2 and CH_4 - with a quality sufficient to obtain information on regional CO_2 and CH_4 sources and sinks. Two satellite instruments deliver the main input data for GHG-CCI: SCIAMACHY/ENVISAT and TANSO-FTS/GOSAT. The first order priority goal of GHG-CCI is the further development of retrieval algorithms for near-surface-sensitive column-averaged dry air mole fractions of CO_2 and CH_4, denoted XCO_2 and XCH_4, to meet the demanding user requirements. GHG-CCI focusses on four core data products: XCO_2 from SCIAMACHY and TANSO and XCH_4 from the same two sensors. For each of the four core data products at least two candidate retrieval algorithms have been independently further developed and the corresponding data products have been quality-assessed and inter-compared. This activity is referred to as "Round Robin" (RR) activity within the CCI. The main goal of the RR was to identify for each of the four core products which algorithms should be used to generate the Climate Research Data Package (CRDP). The CRDP will essentially be the first version of the ECV GHG. This manuscript gives an overview of the GHG-CCI RR and related activities. This comprises the establishment of the user requirements, the improvement of the candidate retrieval algorithms and comparisons with ground-based observations and models. The manuscript summarizes the final RR algorithm selection decision and its justification. Comparison with ground-based Total Carbon Column

Observing Network (TCCON) data indicates that the "breakthrough" single measurement precision requirement has been met for SCIAMACHY and TANSO XCO_2 (< 3 ppm) and TANSO XCH_4 (< 17 ppb). The achieved relative accuracy for XCH_4 is 3-15 ppb for SCIAMACHY and 2-8 ppb for TANSO depending on algorithm and time period. Meeting the 0.5 ppm systematic error requirement for XCO_2 remains a challenge: approximately 1 ppm has been achieved at the validation sites but also larger differences have been found in regions remote from TCCON. More research is needed to identify the causes for the observed differences. In this context GHG-CCI suggests taking advantage of the ensemble of existing data products, for example, via the EnseMble Median Algorithm (EMMA).

Keywords: SCIAMACHY, GOSAT, Greenhouse gases, Carbon dioxide, Methane, Climate Change

1. Introduction

Carbon dioxide (CO_2) is the most important anthropogenic greenhouse gas (GHG) contributing to global warming (Solomon et al., 2007). Despite its importance, our knowledge of the CO_2 sources and sinks has significant gaps (e.g., Stephens et al., 2007, Canadell et al., 2010) and despite efforts to reduce CO_2 emissions, atmospheric CO_2 continues to increase at a rate of approximately 2 ppm/year (Figure 1 top panel; see also Schneising et al., 2011, and references given therein; for a detailed discussion of Fig. 1 see Sect. 4). An improved understanding of the CO_2 sources and sinks is needed for reliable prediction of the future climate of our planet (Solomon et al., 2007). This is also true for methane (CH_4, Figure 1 bottom panel). Atmospheric methane levels increased until about the year 2000, were rather stable during ~2000-2006, but started to increase again in recent years (Rigby et al., 2008, Dlugokencky et al., 2009, Schneising et al., 2011, Frankenberg et al., 2011). Unfortunately, it is not well understood why methane was stable in the years before 2007 (e.g., Simpson et al., 2012) nor why it started to increase again at a rate of approximately 7-8 ppb/year (Schneising et al., 2011).

Global satellite observations sensitive to near-surface CO_2 and CH_4 variations can contribute to a better understanding of the regional sources and sinks of these important greenhouse gases. Information on GHG surface fluxes (emissions and uptake) can be obtained by inverse modeling of

surface fluxes (e.g., Chevallier et al., 2007, Bergamaschi et al., 2009), where satellite observations are compared with predictions of a (chemistry) transport model (e.g., Figure 2) and satellite minus model mismatches are minimized by modifying the surface fluxes used by the model. This requires satellite retrievals to meet challenging requirements, as small errors of the satellite-retrieved atmospheric GHG distributions may result in large errors of the inferred GHG surface fluxes (e.g., Meirink et al., 2006, Chevallier et al., 2005). Instead of direct optimization of surface fluxes it is also possible to optimize (other) model parameters used to model the fluxes, as done in Carbon Cycle Data Assimilation Systems (CCDAS) (e.g., Kaminski et al., 2010, 2012) or other approaches (e.g., Bloom et al., 2010).

The goal of the GHG-CCI project is to generate the Essential Climate Variable (ECV) Greenhouse Gases (GHG) as defined by GCOS (Global Climate Observing System): "Distribution of greenhouse gases, such as CO_2 and CH_4, of sufficient quality to estimate regional sources and sinks" (GCOS, 2006). In order to get information on regional GHG sources and sinks, satellite measurements must be sensitive to near-surface GHG concentration variations. Currently only two satellite instruments deliver (or have delivered until recently) measurements which fulfill this requirement: SCIAMACHY on ENVISAT (March 2002 – April 2012) (Bovensmann et al., 1999) and TANSO-FTS on-board GOSAT (launched in January 2009) (Kuze et al., 2009). Both instruments perform (or have performed) nadir observations of reflected solar radiation in the near-infrared/short-wave-infrared (NIR/SWIR) spectral region, covering the relevant absorption bands of CO_2 and CH_4. They also cover the O_2 A-band spectral region to obtain "dry-air columns" needed for computing GHG dry-air column averaged mole fractions and/or to obtain information on clouds and aerosols. These two instruments are therefore the two core sensors used by GHG-CCI and the near-surface-sensitive column-averaged dry air mole fractions of atmospheric CO_2 and CH_4, denoted XCO_2 (in ppm) and XCH_4 (in ppb), are the core data products of GHG CCI. In addition, other sensors or viewing modes are also used (e.g., MIPAS/ENVISAT and SCIAMACHY solar occultation mode for stratospheric CH_4 profiles and IASI/METOP for mid/upper tropospheric CO_2 and CH_4 columns) as they provide additional constraints for atmospheric layers above the planetary boundary layer. The focus of the first two years

of the GHG-CCI project (September 2010 – August 2012) was to develop existing retrieval algorithms further, in order to improve the accuracy of the retrieved GHG data products.

The focus of GHG-CCI lies on ECV Core Algorithms (ECAs) and their core data products XCO_2 and XCH_4, which is also the focus of this manuscript. Other algorithms, referred to as Additional Constraints Algorithms (ACAs), are algorithms to retrieve CO_2 and/or CH_4 information from satellite data which have no or only little near surface sensitivity but are sensitive to GHG variations in upper layers (the ACAs are listed in Table 3 and further discussed in Section 6).

Several existing candidate ECAs were selected at the outset of the project for ongoing development, and have been iteratively improved upon through the course of the algorithm inter-comparison and validation activity. This activity is referred to as "Round Robin" (RR) exercise within the CCI.

The goal of the RR was to determine which ECA performs best to generate a given GHG-CCI core data product. The selected ECAs will be used in the third year of this project to generate the Climate Research Data Package (CRDP), which will essentially be the first version of the ECV GHG. The description of the RR approach and its results is the focus of this manuscript. Note that previous publications focused on individual algorithms and their data product. Only recently have results obtained using different algorithms been compared, most notably by Oshchepkov et al., 2012, for TANSO/GOSAT XCO_2. This manuscript is therefore one of the first focusing on inter-comparisons.

This manuscript is structured as follows: Section 2 presents an overview of the GHG-CCI project followed by a description of the user requirements in Section 3. In Section 4 the retrieval algorithms are briefly described. The main part of this manuscript is Section 5 where the RR approach and its main results are presented and discussed. Section 6 provides a short overview of the Additional Constraints Algorithms (ACAs) also used within GHG-CCI but not the focus of this manuscript. Section 7 gives a short overview of the Climate Research Data Package (CRDP) to be generated using the selected algorithms. A summary and conclusions are given in Section 8.

2. GHG-CCI project overview

The GHG-CCI project covers all aspects needed to generate the ECV GHG and to assess its quality and usefulness. This includes the use of appropriate satellite instruments (primarily SCIAMACHY/ENVISAT and TANSO/GOSAT to generate global XCO_2 and XCH_4 time series), calibration aspects (related to "Level 0-1 processing", primarily for SCIAMACHY), and development and application of retrieval algorithms to convert the satellite-measured spectra into atmospheric CO_2 and CH_4 information ("Level 1-2 processing"). Also included is the analysis of the resulting global data sets, including validation and user assessments, focusing on inverse modeling of regional surface fluxes (i.e., "Level 2-4 processing"). Note that the fluxes (Level 4 products) will most likely be derived from Level 2 data rather than from (spatio-temporally averaged and potentially gap-filled) Level 3 data products, as Level 2 data contain more information than those at Level 3 and usually benefit from better error characterization.

Level 1 data (i.e., geolocated and calibrated radiances) are input data for CCI (i.e., Level 0-1 processing is covered by other projects). SCIAMACHY Level 0-1 processing experts are part of the GHG-CCI team in order to provide expertise and to ensure that the findings of the study feed back to improve future Level 1 data products if necessary. Close links have been established with the GOSAT team at JAXA for GOSAT Level 1 data access, expertise and feedback.

The SCIAMACHY and TANSO Level 1 data products are de-facto used as Fundamental Climate Data Records (FCDRs, see GCOS, 2006) despite the fact that no dedicated inter-calibration or merging efforts are currently foreseen. Consistency between the time series of the two GHG-CCI core satellites is addressed at the level of the Level 2 data products. Ideally, an ECV data product or Thematic Climate Data Record (TCDR) of a given quantity should be a single merged data record obtained from all available appropriate sensors such as SCIAMACHY and TANSO for satellite-derived XCO_2. However, within the present initial stage of this project only first steps in this direction have been carried out (see Section 5).

The ground-based validation of the “satellite-derived” XCO_2 and XCH_4 data products largely relies on the Total Carbon Column Observing Network (TCCON) (Wunch et al., 2010, 2011a) as this network

has been designed and developed for this purpose. Methods to also use data from other sources in the future (e.g., NDACC (see Sussmann et al., 2013), GAW) are being developed in parallel. Aircraft observations, e.g., HIPPO (e.g., Wofsy, 2011, Wecht et al., 2012), are also interesting, but have not yet been used directly (indirectly some of these data have been used via the calibration of TCCON, see Sect. 5.2.1).

A dedicated GHG-CCI Climate Research Group (CRG) has been set up to represent the users of the satellite-derived CO_2 and CH_4 data products and to provide expertise on inverse modeling of surface fluxes, CCDAS and other user related aspects. A strong link exists between GHG-CCI and the EU FP7 GMES project MACC-II (Monitoring of Atmospheric Composition and Climate - Interim Implementation, http://www.gmes-atmosphere.eu/) that provides feedback on the data quality.

Key activities carried out in the first two years of this project were the establishment of the user requirements (Section 3), the further development of retrieval algorithms (described briefly in Section 4) and data processing and data analysis with the goal of identifying which algorithms perform best ("Round Robin" (RR)). The description of these RR activities and their results is the focus of this manuscript (Section 5). In the third year of this project the selected algorithms will be used to generate the CRDP (see Section 7), which will subsequently be validated and assessed by users.

3. User requirements

An important initial activity carried out in this project was the establishment of the user requirements. They have been formulated in detail in the GHG-CCI User Requirements Document (URD) (Buchwitz et al., 2011a). The requirements are based on peer-reviewed publications primarily prepared in the context of existing or planned satellite missions and GHG-CCI CRG user expertise and experience with existing satellite data.

Most critical are the requirements on random and systematic errors listed in Table 1. The most challenging requirement is the one on biases for XCO_2. The threshold requirement is 0.5 ppm because even errors of a few tenths of a ppm can result in large errors of the inferred CO_2 surface fluxes when used as input data for inverse modeling schemes (e.g., Chevallier et al., 2005). However, to what

extent systematic errors result in biases of the inferred fluxes depends on the spatio-temporal pattern of the systematic errors. A global bias, even if considerably larger than the required 0.5 ppm, would not be critical because it can easily be detected and corrected *ad hoc*. Most critical are state-dependent systematic errors, which result in regional-scale (~1000 km) biases on medium time scales (~ monthly), because they will likely be missed by bias-correction schemes. As the overall impact of the atmospheric concentration error on the surface flux error depends on the spatio-temporal pattern of the concentration error, the values listed in Table 1 have to be interpreted with care. The requirements reflect what the GHG-CCI users would like to see achieved. The utility of the data can ultimately only be determined by careful analysis. The numbers listed in Table 1serve to give a rough indication of the required uncertainties but should not be over-interpreted.

The requirements for XCH_4 are also challenging but somewhat less demanding than those for XCO_2. The main reason is that XCH_4 is more variable compared to XCO_2 relative to its background value on the spatio-temporal scales relevant for the satellite retrievals (e.g, Frankenberg et al., 2005, 2011, Meirink et al., 2006, Bergamaschi et al., 2009, Schneising et al., 2011, 2012).

4. Retrieval algorithms

In this section, a brief overview of each retrieval algorithm used for the GHG-CCI RR is given. The reader is referred to peer-reviewed publications for details. All algorithms used within the GHG-CCI RR are also described in the GHG-CCI Algorithm Theoretical Basis Document (ATBD) (Reuter et al., 2012a).

The ECV Core Algorithms (ECAs) generate one or more of the four GHG-CCI core data products, XCO_2 (in ppm) and XCH_4 (in ppb) from SCIAMACHY and TANSO (each of the four combinations is a separate product). An overview of these algorithms is given in Table 2 and briefly described in the following sub-sections. Results obtained with all ECAs are shown in Fig. 1: the top panel shows northern hemispheric (NH) time series of XCO_2 and the bottom panel XCH_4 time series. As can be seen, the various XCO_2 time series (generated with the various algorithms described in the following sub-sections) are similar but not exactly identical. There are clear differences, e.g., a difference of the seasonal cycle amplitude, between the two SCIAMACHY algorithms WFMD (Schneising et al., 2011,

217 Heymann et al., 2012b) and BESD (Reuter et al., 2011) likely due to sub-visual cirrus clouds not
218 explicitly considered by WFMD. Differences are also due to the different spatial sampling of the
219 various data products. From Figure 1 it can therefore typically not be concluded which data product is
220 the most accurate. This requires, for example, a careful comparison with independent accurate ground-
221 based observations (see Section 5.2). However, one obvious problem can be identified: the
222 SCIAMACHY XCH_4 product generated with the IMAP algorithm (Frankenberg et al., 2011) suffers
223 from a significant high bias (relative to several other TANSO/GOSAT XCH_4 data products) during the
224 year 2010 (highlighted by the dotted line). This problem is related to SCIAMACHY detector
225 degradation issues which are not yet properly dealt with by the SCIAMACHY radiometric calibration
226 nor compensated by the IMAP algorithm (note that the second SCIAMACHY XCH_4 algorithm
227 WFMD (Schneising et al., 2011) has not yet been applied to 2010 data; the WFMD time series covers
228 only the years 2003-2009). As will be discussed in more detail below, the most challenging problems
229 addressed within GHG-CCI are related to achieving the required accuracy: for XCO_2 this is a
230 challenge because of demanding user requirements and for XCH_4 the most important challenge was to
231 deal with the progressive SCIAMACHY detector degradation in the spectral region needed for
232 methane retrieval which started in October 2005 (see Schneising et al., 2011, and Frankenberg et al.,
233 2011, for a detailed discussion).

234 **4.1 Full Physics (FP) and Proxy (PR) algorithms**

235 Within GHG-CCI, two types of ECAs can be distinguished: The “Full Physics” (FP) algorithms and
236 the light path “Proxy” (PR) algorithms (see also Schepers et al., 2012).

237 FP algorithms model all relevant physical effects such as scattering by aerosols and clouds and have
238 corresponding elements as part of the state vector, which contains all parameters which are to be
239 retrieved. The FP algorithms obtain the dry air column-averaged mole fraction (needed to compute the
240 dry air column-averaged mole fractions of the GHG, i.e., XCO_2 and/or XCH_4) either from the
241 retrieved surface pressure or using meteorological information.

The PR algorithms are based on computing the dry air column-averaged mole fraction using a "reference gas", which has to be much less variable than the gas of interest on the relevant spatio-temporal scales. The PR method is used for XCH_4 retrieval using CO_2 as a reference gas. The XCH_4 is essentially obtained from computing the ratio of the retrieved CH_4 column and the retrieved CO_2 column. The advantage of this method is that it is potentially very fast, accurate and robust (as several systematic errors cancel in the CH_4/CO_2 column ratio). The disadvantage is that a correction is needed for CO_2 variability, typically based on a global model (see, e.g., Frankenberg et al., 2005, 2011, Parker et al., 2011, Schneising et al., 2009, 2011, Schepers et al., 2012).

4.2 SCIAMACHY XCO_2 algorithms

The Weighting Function Modified (WFM) Differential Optical Absorption Spectroscopy (DOAS) algorithm (WFM-DOAS or WFMD) has been developed to retrieve vertical columns of several atmospheric gases including the GHGs discussed in this manuscript (Buchwitz et al., 2000). During the last decade, this algorithm has been significantly improved and used to generate global multi-year XCO_2 and XCH_4 data sets from SCIAMACHY (Buchwitz et al., 2005, 2007; Schneising et al., 2008, 2009). Within GHG-CCI, WFMD has been further improved and used to generate long-term consistent time series (Schneising et al., 2011, 2012, Heymann et al., 2012a, 2012b). WFMD has been implemented as a fast look-up table (LUT) based retrieval scheme to avoid time consuming radiative transfer (RT) simulations. WFMD is a least-squares method using a single constant atmospheric prior (e.g., single constant CO_2 and CH_4 mixing ratio profiles, a single aerosol scenario, no clouds). WFMD can process one orbit of SCIAMACHY observations in a few minutes on a single workstation. Aerosols and cirrus clouds are only treated approximately by considering spectrally broad band effects by a low-order polynomial and by post-processing filtering. Overall, this results in small but significant biases, especially for XCO_2 (Heymann et al., 2012a). Recently, an improved version of WFMD has been developed for SCIAMACHY XCO_2 retrieval (Heymann et al., 2012b, see also Figure 2) and the XCO_2 data set generated with this latest version has been used for the GHG-CCI RR. For SCIAMACHY XCH_4 retrieval, the WFMD version described in Schneising et al., 2011, 2012, has been used (see below).

The Bremen Optimal Estimation DOAS (BESD) FP algorithm was specifically developed for accurate and precise SCIAMACHY XCO_2 retrieval considering aerosols and clouds thereby overcoming limitations of the WFMD algorithm (Reuter et al., 2010, 2011). In contrast to WFMD, BESD is not based on a LUT scheme but uses on-line RT model simulations. BESD is therefore computationally much more demanding. Also, unlike WFMD, BESD is based on Optimal Estimation (OE, Rodgers, 2000) and aerosol and cirrus parameters are state vector elements and retrieved in addition to XCO_2.

4.3 TANSO XCO_2 algorithms

Both GHG-CCI TANSO XCO_2 retrieval algorithms are FP algorithms: the University of Leicester's (UoL) OCO (Orbiting Carbon Observatory, Crisp et al., 2004) FP ("UoL-FP" or OCFP) algorithm (Cogan et al., 2012, Parker et al., 2011) and the RemoteC (or SRON Full Physics (SRFP)) algorithm (Butz et al., 2011). Both algorithms are based on adjusting parameters of a surface-atmosphere state vector and other parameters to the satellite observations, but differ in many details (different RT models, different inversion schemes (OE or Tikhonov-Phillips), different schemes for aerosol modeling and inversion, use of different pre-processing and post-processing steps, etc.) as discussed in Cogan et al., 2012, Parker et al., 2011, and Butz et al., 2011.

4.4 SCIAMACHY XCH_4 algorithms

For SCIAMACHY XCH_4 retrievals, PR algorithms are used: WFMD (Schneising et al., 2011, see above) and IMAP (Iterative Maximum A Posteriori) DOAS (Frankenberg et al., 2011). These algorithms were already well developed when GHG-CCI started but had essentially only been applied to retrieve XCH_4 from the first three years of the ENVISAT mission (e.g., Schneising et al., 2008). Within GHG-CCI, this time series has been significantly extended. The key challenge was (and partly still is, see Figure 1) to deal with the significant detector degradation in the spectral region needed for methane retrievals after 2005 (see Frankenberg et al., 2011, and Schneising et al., 2011, for details).

4.5 TANSO XCH_4 algorithms

To overcome the key limitation of the XCH_4 PR algorithms, namely the need to correct the retrieved XCH_4 for CO_2 variations using a model, FP algorithms are also used within GHG-CCI, but only for TANSO. TANSO has higher spectral resolution than SCIAMACHY which is exploited to also retrieve scattering parameters in addition to CH_4. Two TANSO XCH_4 FP retrieval algorithms are being used within GHG-CCI, which are also used for TANSO XCO_2 retrieval (see above), OCFP (Parker et al., 2011) and SRFP (Butz et al., 2011), in addition to the two PR algorithms OCPR (Parker et al., 2011) and SRPR (Schepers et al., 2012).

5. Round Robin approach and results

In this section an overview of the GHG-CCI Round Robin (RR) activities is given which have been carried out in the first two years of this project.

5.1 Round Robin approach

The ultimate goal of the GHG-CCI RR was to identify which algorithms and corresponding data products to use for generating the CRDP. This comprised the further development of existing retrieval algorithms with the goal of meeting the challenging user requirements, the application of these algorithms to generate global multi-year XCO_2 and XCH_4 sets, the comparison with ground-based reference data and inter-comparisons of the data products generated with the competing ECAs.

The selection procedure for ECAs and ACAs is described in the GHG-CCI Round Robin Evaluation Protocol (RREP, Buchwitz et al., 2011b). Initially the plan was to develop a score-based selection scheme, i.e., to compute a single number for each algorithm / data product (the higher the number, the better the algorithm), mainly based on satellite – ground-based observation differences. However, this was not pursued because a scientifically sound basis for the classification could not be established. Instead a set of Figures of Merit (FoM), mostly based on differences between satellite and ground-based observations, have been defined (see RREP, Buchwitz et al., 2011b) and evaluated. However, as explained in the RREP and also shown in this manuscript, the comparison with the ground-based observations is only one component for the final selection primarily because of the sparseness of the

ground-based network (see Section 5.2). Another major component of the selection procedure was the analysis of (global and regional) maps and time series, including comparisons with global state-of-the-art models, and inter-comparisons of the data products generated with the different candidate algorithms. Note that "blind testing" has not been used as it would have been possible to identify the algorithms/products by using some of their characteristics such as averaging kernels and spatial coverage. Some key results of this RR activity are presented here including a summary of the main RR decision results given in Section 5.6 for ECAs and Section 6 for ACAs.

According to the initial ESA specification of the CCI RR exercise it was required to evaluate "algorithms". However, complex algorithms such as the ones used within GHG-CCI can hardly be evaluated, especially not in terms of identifying "the best one" in terms of smallest biases when applied to real data. Simulated retrievals have been performed (see, e.g., Buchwitz et al., 2011c, 2012a, and references given therein) but only for the individual algorithms and not in a consistent manner. This would have been a major activity incompatible with the CCI schedule especially if the goal would have been to obtain a better understanding of the differences between the data products obtained from the real observations. In this context it has not been identified that any of the algorithms suffer from obvious shortcomings. All XCO_2 algorithms, for example, use different approaches to mitigate biases due to scattering by aerosols and (thin) clouds, but it is virtually impossible to identify *a priori*, e.g., based on a description of the algorithms and the simulation results, which of the approaches will result in the smallest XCO_2 or XCH_4 biases when applied to real data.

What has been evaluated in detail are the end products, i.e., the quality of the XCO_2 and XCH_4 data products. This means that primarily data products have been evaluated during RR but not algorithms. As shown in this manuscript, this is not a trivial task, e.g., due to the sparseness of the TCCON reference data. Therefore, as shown in this manuscript, the RR decisions are not only based on comparisons with TCCON. The satellite retrieval team focused on producing the best possible end products. Which input data to use and how to treat them, e.g., in a dedicated pre-processing step, has not been prescribed. Pre-processing steps may be critical for the quality of the end product. This is particularly true if the instrument shows significant degradation as is the case for SCIAMACHY after

2005 especially in the spectral region needed for methane retrieval. To deal with this, quite different approaches have been used by the two algorithms IMAP (Frankenberg et al., 2011) and WFMD (Schneising et al., 2011, 2012). For example, IMAP uses as input data spectra that have been specifically calibrated at SRON and IMAP also uses a single so-called "Dead and Bad detector Pixel Mask" (DBPM), needed to reject detector pixels which are not useful. In contrast, WFMD uses the official standard SCIAMACHY Level 1 data product with standard calibration and several DBPMs, each optimized for a certain time period, typically covering one or more years (see Schneising et al., 2011, for details).

Finally, it is important to highlight the preliminary nature of the RR. This is due to the fact that all Level 1 input data and retrieval algorithms are continuously being improved. An algorithm / data product currently identified to be the best one will not necessarily be the best one in the future. GHG-CCI therefore needs to be flexible and will aim to consider this in future phases of the CCI.

5.2 Comparison with ground-based (TCCON) observations

5.2.1 TCCON data and error characteristics

The most relevant ground-based observations for the validation of the satellite-derived XCO_2 and XCH_4 data products are the corresponding data products of the TCCON. The TCCON data products have been obtained from the TCCON website (www.tccon.caltech.edu/; latest access Feb. 2012 using version GGG2009, i.e., not the latest version GGG2012, which was not available for the GHG-CCI Round Robin comparison) or have been provided by the TCCON PIs. The TCCON products have been calibrated to WMO/GAW in situ trace gas measurement scales using aircraft observations (Wunch et al., 2010, Deutscher et al., 2010, Geibel et al., 2012, Messerschmidt et al., 2012). The best independent estimates of the TCCON inter-site comparability to date are provided by these independent aircraft calibration data. While not exhaustive, these demonstrate consistency at the 0.1% level (1-sigma) for XCO_2 (~0.4 ppm) and 0.2% for XCH_4 (~4 ppb), with no obvious inter-hemispheric differences (Wunch et al., 2010). Nevertheless, the TCCON team recognizes that inter-site comparability needs to be better characterized, especially for methane (e.g., at Darwin and Wollongong, not discussed in the references cited above), and work is in progress to achieve this. The

372 systematic and random errors of single TCCON data are therefore typically 0.4 ppm for XCO_2 (1-
373 sigma) and 4 ppb (1-sigma) for XCH_4 (Notholt et al., 2012, based on Wunch et al., 2010). Due to these
374 errors of the TCCON data (but also for other reasons, e.g., non-perfect spatio-temporal co-location)
375 the estimated systematic and random errors of the satellite retrievals as reported here have to be
376 interpreted as upper limit estimates, i.e., the satellite data errors are likely smaller than reported here.

377 **5.2.2 Inter-comparison method**

378 Different inter-comparison methods have been used, e.g., to ensure robustness of the findings. In
379 addition to the method used and results obtained by the validation team (Notholt et al., 2012), which
380 are summarized in this manuscript, independent inter-comparisons of the satellite data products with
381 TCCON have also been carried out by the satellite data product provider (Buchwitz et al., 2012a). The
382 methods differ by various aspects such as investigated time period and direct comparison or
383 comparison after transformation to common *a priori* profiles and application of averaging kernels.
384 Each satellite data product provider performed an independent validation of his data product
385 (considering averaging kernels or not) covering the entire time series (to the extent possible given the
386 limitations of the TCCON data, see Tab. 4). In contrast, the validation team has applied the same
387 method to all satellite data products and has, for a given product, only used a time period where data
388 from all competing algorithms were available (SCIAMACHY: XCO_2: 2006-2009; XCH_4: 2003-2009,
389 TANSO: mid 2009-2010).

390 The method used by the validation team is based on a direct comparison of the co-located satellite and
391 TCCON data products. No correction for different *a priori* profiles and averaging kernels has been
392 applied. Note that it is not trivial to consider averaging kernels for the XCO_2 and XCH_4 satellite and
393 TCCON retrievals as strictly speaking this requires a reliable estimate of the real atmospheric
394 variability, which is unknown. This aspect is discussed in detail in Wunch et al., 2011b, where the
395 impact of this correction for TANSO XCO_2 is discussed at Lamont, USA, where the real variability of
396 the CO_2 profiles is obtained using regular aircraft and other observations. For the global data sets this
397 is not possible. Nevertheless, for some of the satellite products, averaging kernels have been applied
398 by the satellite data provider. For example, Reuter et al., 2013, has applied individual averaging

399 kernels for all XCO_2 products from SCIAMACHY and TANSO by adjusting all retrievals to a
400 common *a priori* using the Simple Empirical CO_2 Model (SECM) described in Reuter et al., 2012b.
401 They found that the adjustments are typically a few tenth of a ppm. Reuter et al., 2012b, estimated the
402 smoothing errors and found that it is typically 0.17 ppm for SCIAMACHY XCO_2 and 0.05 ppm for
403 TCCON XCO_2. These results indicate that the impact of applying or not applying the averaging
404 kernels for satellite – TCCON comparisons is small. The reason is that the averaging kernels of the
405 TCCON and the satellite data are close to unity and the resulting smoothing error is therefore typically
406 quite small, especially for XCO_2. For methane the (relative) smoothing errors are somewhat larger, as
407 methane is more variable. For example, Parker et al., 2011, found that "the mean smoothing error
408 difference included in the GOSAT to TCCON comparisons can account for 15.7 to 17.4 ppb for the
409 northerly sites and for 1.1 ppb at the lowest latitude site". For the SCIAMACHY XCH_4 validation
410 results presented in Schneising et al., 2012, it has been found that applying averaging kernels (by
411 using TM5 model profiles as a common *a priori*) leads to adjustments of 0.4% (approx. 7 ppb).
412 Overall it has been found that the validation results obtained by the validation team (Notholt et al.,
413 2012) and the satellite data provider (Buchwitz et al., 2012a), where averaging kernels have been
414 applied for at least some of the products, agree well, especially for XCO_2 (Buchwitz et al., 2012b).
415 The comparison of the various methods used to quantify random and systematic errors of the satellite
416 products (Buchwitz et al., 2012b) indicates that the RR validation results are robust.

417 In the following, the results obtained by the validation team are presented. Detailed results will be
418 reported elsewhere (Dils et al., manuscript in preparation, preliminary title: "The Greenhouse Gas
419 Climate Change Initiative (GHG-CCI): Comparative validation of SCIAMACHY and TANSO-FTS
420 CO_2 and CH_4 retrieval algorithm products with measurements from the TCCON network"). Therefore
421 we here give only a short overview highlighting major findings.

422 For each product and each TCCON site a number of Figures of Merit (FoMs) have been computed by
423 the validation team. Key results are shown in Fig. 3 for XCO_2 and Fig. 4 for XCH_4., discussed in detail
424 in dedicated sub-sections below. Shown are comparisons of the four GHG-CCI core data products
425 generated with two or more of the candidate algorithms at the 10 TCCON sites listed in Table 4. The

results shown in Figs. 3 and 4 have been generated using a spatio-temporal co-location criterion of 2 hours and 500 km (for alternative co-location criteria see Notholt et al., 2012). Several numerical values are given, which are also listed in Table 5, computed from satellite minus TCCON differences for each single satellite retrieval and the corresponding TCCON mean value. On the left hand side of Figs. 3 and 4 the mean satellite-TCCON differences are shown for each of the 10 TCCON sites and all four core data products and their corresponding ECAs. For each ECA the standard deviation of the station-to-station bias has been computed ("StdDev") and the total number of co-located satellite retrievals used for comparison ("N"). The standard deviation of the station-to-station bias is interpreted as a relevant measure of the systematic error ("relative accuracy" or "relative bias"). The standard deviation is more relevant to characterize systematic errors compared to, for example, the mean difference. Most critical is to achieve high "relative accuracy" (or low "relative bias") not necessarily high "absolute accuracy" (although this would of course be better). For example, a constant offset of the satellite data would not be critical if the data are being used for surface flux inverse modeling (see Section 3) and this is considered by computing the standard deviation. On the right hand side of Figs. 3 and 4 the standard deviations of the satellite-TCCON differences are shown for each TCCON site. They are a measure of the random error (scatter) of the satellite retrievals. The corresponding mean value over all TCCON sites is used to characterize the mean random error (or "precision") of the corresponding satellite data product. In the following, Figs. 3 and 4 are discussed in more detail for each of the products.

5.2.3 Satellite XCO_2 comparisons with TCCON

The comparison of the two SCIAMACHY XCO_2 retrieval algorithms WFMD and BESD with TCCON shows the following (Figure 3, top half): BESD has typically lower systematic errors (0.7 ppm) compared to WFMD (1.3 ppm) and also a higher precision (2.3 ppm compared to 5.1 ppm). Ultimately it can be expected that the biases of BESD will be even lower as it has been identified (not shown) that the BESD RR data set suffers from problems related to the SCIAMACHY Level 1 data product used (version 7 consolidation level u, "L1v7u"). This data product was used because it was the latest version available when the final RR data set had to be generated and because it also covers the

time period after 2009. The previous Level 1 version 6 (L1v6), used by WFMD, does not suffer from these problems but is only available until the end of 2009, where the WFMD data set ends. It has been found that BESD retrievals for selected months using the improved new version L1v7w have much lower biases especially because the many outliers caused by the L1v7u spectra are not present any more (not shown). It is therefore necessary and planned to reprocess the entire SCIAMACHY data set with BESD using L1v7w, e.g., for the generation of the CRDP. A potentially important pro for WFMD for certain applications is the much larger number of data points.

The comparison of the two TANSO XCO_2 retrieval algorithms OCFP and SRFP with TCCON shows the following (Figure 3, bottom half): The biases depend on site and are typically in the range +/- 1 ppm. They are very similar for both algorithms. This is also true for the standard deviation of the difference between the TANSO and TCCON estimates, which is typically in the range 2-3 ppm. The number of co-locations is also nearly identical for both algorithms but varies significantly from site to site, which is true for all comparisons shown in Figs. 3 and 4.

As shown in Table 5, the precision requirement for XCO_2 is met by all algorithms. WFMD meets the threshold requirement and the other algorithms including BESD even meet the breakthrough requirement. The challenging 0.5 ppm bias requirement has however not yet been met but several algorithms achieve a performance close to the threshold requirement (0.6-0.9 ppm, depending on algorithm).

5.2.4 Satellite XCH_4 comparisons with TCCON

The comparison of the two SCIAMACHY XCH_4 retrieval algorithms WFMD and IMAP with TCCON shows the following (Figure 4, top half): Overall, the systematic differences with respect to TCCON vary from site to site from nearly 0 ppb at Lamont to 20-30 ppb at the southern hemisphere (SH) sites Darwin, Wollongong, and Lauder, but are very similar for WFMD and IMAP. The reason for the large differences at these SH sites have not yet been identified. This is probably not due to the TCCON reference data as these differences are larger than the estimated TCCON inter-site comparability (see Sect. 5.2.1) and also the comparison with TANSO XCH_4 (see below) does not show this type of systematic deviation (the OCFP results however also show a low bias at the SH sites

compared to the northern sites esp. at Darwin). Agreement is within +/- 10 ppb if these SH sites are excluded. In order to obtain an estimate of the relative biases (i.e., considering that an overall offset is not critical), the standard deviation of the station-to-station biases has been computed: it amounts to 11 ppb for WFMD and 15 ppb for IMAP. The standard deviation of the satellite-TCCON differences, which is a measure of the single measurement precision (1-sigma), is on average 82 ppb for WFMD and 50 ppb for IMAP. Because nearly all TCCON sites started operation after 2005 (see Table 4), i.e., after the loss of important SCIAMACHY methane detector pixels due to detector degradation, the values listed for SCIAMACHY in Figure 4 are not representative for the years 2003-2005. Until the end of 2005 the performance was much better and the corresponding values are listed in curved brackets in Table 5. A possible explanation for the larger scatter (worse precision) of WFMD after 2005 is that WFMD is an unconstrained least-squares algorithm whereas IMAP is based on Optimal Estimation and uses detailed CH_4 information (as a function of latitude, altitude and time but not longitude) from a global model as *a priori* information. This raises the question why the precision of the two data products is similar for 2003-2005. This could be related to the fact that only a single DBPM is used by IMAP whereas WFMD has used a DBPM optimized for 2003-2005. Another possible explanation could be the use of differently calibrated input data. As shown in Fig. 4, the number of satellite soundings used varies significantly from site to site, but overall is very similar for WFMD (N=37628) and IMAP (39489) (at least at TCCON sites, for other locations this may not be true, see Figures 9 and 10).

The comparison of the four TANSO XCH_4 retrieval algorithms (OCPR, OCFP, SRPR, SRFP) with TCCON shows the following (Figure 4, bottom half): The biases depend on the TCCON site but are in the range +/- 15 ppb. The estimated relative bias is best for OCPR (2 ppb) and worst for OCFP (8 ppb). OCPR has the largest number of data points (followed by SRPR). The number of data points is higher for the PR algorithms (OCPR and SRPR) compared to the FP algorithms (OCFP and SRFP). The FP algorithm with the lowest relative bias is SRFP (3 ppb). The PR algorithm with the lowest relative bias is OCPR (2 ppb). The standard deviation of the satellite – TCCON differences are nearly identical for all four algorithms.

As shown in Table 5, the SCIAMACHY XCH_4 product for 2003-2005 meets the threshold precision requirement (but not for 2006 and later years due to the detector degradation). In contrast, the TANSO XCH_4 has a much higher precision and even the breakthrough precision requirement is met by all algorithms. All TANSO XCH_4 algorithms meet the relative accuracy (relative bias) user requirement - some are close to or even better than the goal requirement. For SCIAMACHY this is only true for 2003-2005.

Concerning the final RR algorithm selection decision, it is important not to over-interpret the numerical values listed in Table 5 due to the sparseness of the TCCON sites. For this and other reasons, the TCCON comparisons presented and discussed in this section are only one key component of the GHG-CCI RR activities. Therefore, more comparisons have been conducted, for XCO_2 and XCH_4, as described in the following.

5.3 Inter-comparison of XCO_2 data products

Within GHG-CCI two algorithms have been further developed to retrieve XCO_2 from SCIAMACHY, namely WFMD and BESD, and two algorithms to retrieve XCO_2 from TANSO, namely OCFP and SRFP. In addition, there are three non-European TANSO algorithms presented and discussed in the peer-reviewed literature whose data products have also been used for comparison: (i) the official operational TANSO algorithm (v02.xx) developed at the National Institute for Environmental Studies (NIES) in Japan (Yoshida et al., 2011; in the following referred to as "NIES" algorithm), (ii) a scientific algorithm called PPDF (Pathlength Probability Density Function) also developed at NIES (Bril et al., 2007, Oshchepkov et al., 2008, 2009, 2011, 2012), and (iii) NASA/JPL's ACOS (Atmospheric CO_2 Observations from Space) v2.9 algorithm (O'Dell et al., 2012, Crisp et al., 2012).

The global XCO_2 data products from all 7 algorithms have been inter-compared within GHG-CCI (Reuter et al. 2013, Buchwitz et al., 2012a). The analysis revealed the following: The various satellite XCO_2 data products all capture the expected large scale variations of atmospheric CO_2 such as the time dependent north-south gradient (Figures 5 and 6, discussed below) and the CO_2 increase and seasonal cycle (Figure 1) but exhibit differences in the spatio-temporal pattern which – depending on region and time – may exceed the relative bias user requirement of 0.5 ppm.

Typical examples are shown in Figures 5 and 6. Figure 5 shows comparisons of the four GHG-CCI XCO_2 algorithms (BESD, WFMD, SRFP, OCFP). Figure 6 shows the GHG-CCI algorithms as well as the three non-European algorithms mentioned above (ACOS (v2.9), PPDF (NIES PPDF-D), and NIES (v02.xx)) for the two months September 2009 and May 2010. Also shown is the ensemble data product generated with the EnseMble Median Algorithm (EMMA) algorithm, discussed below, TCCON XCO_2, and XCO_2 from NOAA's CO_2 assimilation system CarbonTracker (CT) (Peters et al., 2007). As can be seen, all satellite retrieval algorithms capture the north-south XCO_2 gradient, which is significantly different for the two months shown, in good to reasonable agreement with TCCON and CarbonTracker (Figure 6). As can also be seen, differences between the data products often exceed 0.5 ppm, particularly at locations remote from TCCON sites (e.g., Sahara, South America, Africa). As discussed in Section 5.2, it appears virtually impossible to use TCCON to determine which algorithm performs best, at least for TANSO. For SCIAMACHY it has been shown that BESD outperforms WFMD in terms of single measurement precision and bias not however in terms of number of observations, which is significantly higher for WFMD. It is also likely that a "best data product" for all conditions does not exist at present as each retrieval algorithm is expected to have its strengths and weaknesses. Therefore, which algorithm performs best may depend on the spatio-temporal interval of interest. Clearly, more research is needed to understand the differences between the various XCO_2 data sets shown in Figures 5 and 6. One approach to further assess the relative quality of the various satellite-derived global XCO_2 data sets is to compare them with their median. This approach is presented in the following section.

5.3.1 Comparison with ensemble median (EMMA)

In this section we aim at answering two related questions: (i) How to determine which data product is likely "the best", if the largest differences are at locations remote from validation sites? (ii) Which data product should be used for inverse modeling of surface fluxes if all products differ and if it is not clear which product would give the most reliable results? To answer these questions we use the median of the various XCO_2 products. The situation appears to be similar to that for climate modeling: it is not clear which "model" is the best and (remote from validation sites) there is no truth to compare with. A

promising approach to deal with this is to make use of the fact that several state-of-the-art algorithms and corresponding XCO_2 data products are available, i.e., an ensemble of data products, which can be exploited. This is the underlying idea of the EnseMble Median Algorithm (EMMA, Reuter et al., 2013). As described in more detail below and in Reuter et al., 2013, EMMA computes the median of an ensemble of individual XCO_2 data products, which can be used for comparison with the individual data products, e.g., to identify outliers. However, the EMMA XCO_2 product has also been generated to be useful as a stand-alone XCO_2 data product for inverse modeling and other applications.

The strength of using an ensemble of satellite data products was highlighted at the end of the first year of the GHG-CCI project (Buchwitz et al., 2011c), when biases (0.5%) between Bialystok TCCON XCO_2 and co-incident satellite data were identified in the majority of algorithms participating in the GHG-CCI. This bias occurred due to an empirical correction of known magnitude, to account for a laser-sampling bias in the FTS data before September 21, 2009, inadvertently being applied in the wrong direction. A bias in XCH_4 in the early part of the Bialystok time series that occurred due to missing fits in one of the CH_4 micro-windows was also brought to light by comparisons to the ensemble of satellite retrievals. The identification and quantification of these biases would most likely not have been possible with a single algorithm / data product, due to difficulty in proving that such relatively small differences are not due to possible retrieval algorithm issues.

A detailed description of EMMA is presented in Reuter at al., 2013. Therefore here only a short overview is given. The presented version of EMMA (v1.3a) uses the 7 individual satellite XCO_2 products shown in Figs. 6 and 7 and generates a Level 2 product (i.e., a product containing the XCO_2 of the individual satellite soundings including uncertainty estimate and other information such as averaging kernels) using the median in each 10^ox10^o monthly grid cell ("voxel"). In short, EMMA works as follows: For each voxel, the mean XCO_2 value is computed for each of the 7 individual data products. The median of the 7 mean values determines which of the individual satellite Level 2 data products is used for the EMMA data product for that voxel (if a certain voxel is not covered by all 7 data products, a smaller number of data products is used). Using the median has several advantages compared to, for example, using the mean value. A key aspect is that the median is robust with respect

588 to outliers. Using the median essentially removes outliers. This is of critical importance as each of the
589 individual data products appears to suffer from outliers but where they appear and when is not known
590 *a priori* and depends on the algorithm. Of at least equal importance is that the GHG-CCI users need a
591 Level 2 data product (individual soundings) and not a Level 3 data product (e.g., gridded monthly
592 averages). Furthermore, the use of an ensemble of data products possibly permits the generation of
593 more reliable uncertainty estimates, obtained from a combination of the ensemble scatter and the
594 reported uncertainties of the individual algorithms (which are primarily estimates of the random
595 uncertainty). This would in particular be important to get a handle on the systematic error component
596 of the uncertainty, which is very difficult (if not impossible) to reliably quantify for each algorithm
597 individually. For an ensemble, this would strictly speaking require that the median is bias free which is
598 unlikely to be the case. Nevertheless, the spatio-temporal intervals where the various data products
599 disagree are very likely intervals where the data products need to be used with care. In any case,
600 reliable XCO_2 error estimates of the satellite retrievals are of critical importance for the user of the
601 GHG-CCI atmospheric data products.

602 Figures such as Figure 6 also permits the determination of which of the data sets agree and which
603 disagree. For example, the EMMA product, but also most of the individual TANSO products and
604 SCIAMACHY/BESD, agree well or at least reasonably with each other as well as with TCCON and
605 CarbonTracker (see green and yellow smileys), whereas this is not always true for the two very fast
606 algorithms WFMD and PPDF (see red smileys). Figure 7 shows pie charts indicating the overall
607 agreement and disagreement of each of the individual algorithms with the median. The results are
608 consistent with the already reported findings, e.g., better performance of BESD compared to WFMD
609 and similar performance of the TANSO XCO_2 algorithms.

610 A large number of other comparisons of the individual data products and the EMMA product with
611 TCCON but also with CarbonTracker have been carried out. Figure 8 shows, as an example, a
612 comparison of the amplitude of the XCO_2 seasonal cycle. As can be seen, all satellite data shown
613 suggest that the seasonal cycle is underestimated by CarbonTracker by ~1.5 +/- 0.5 ppm peak-to-peak.
614 Using only a single data product it would be difficult to “prove” that such a relatively small difference

615 (~0.3% of the total column) is significant and not caused by or at least significantly influenced by
616 retrieval issues (see, e.g., the discussion given in Schneising et al., 2011, on this topic). Using an
617 ensemble of data products based on more than one satellite and using several essentially independent
618 algorithms allows one to draw more confident conclusions with respect to the interpretation of satellite
619 – model XCO_2 differences than would be possible using a single data product only. Within GHG-CCI
620 it is therefore planned to continue the efforts on EMMA in addition to further developing the
621 individual algorithms.

622 **5.4 Inter-comparison of SCIAMACHY XCH_4 data products**

623 The multi-year global retrievals obtained from the two SCIAMACHY XCH_4 algorithms, WFMD and
624 IMAP, have been compared with one another. Figure 9 shows, as a typical example, a comparison of
625 one month (August 2005) of the global WFMD and IMAP data products (Figure 10 shows the
626 corresponding results for July 2009; results for other months are shown in Buchwitz et al., 2012a). As
627 can be seen, the monthly XCH_4 maps generated with the two algorithms show – depending on region -
628 similar but also significantly different patterns. Both maps show higher methane concentrations over
629 the Northern Hemisphere (NH), where most of the methane sources are located, compared to the
630 Southern Hemisphere (SH). Both data sets agree reasonably well (within typically +/- 10 ppb) over
631 most parts of the SH land areas but over some areas WFMD XCH_4 can be up to approximately 20 ppb
632 higher. Over the NH the situation appears to be more complex. Both data sets show elevated methane
633 over large parts of China, south-east Asia and India, but the patterns are not identical, with WFMD
634 being higher over south-east Asia and lower over parts of India compared to IMAP. WFMD and
635 IMAP not only use differently calibrated input data (standard versus non-standard calibration) and
636 different retrieval methods (least squares versus OE), but also different post-processing quality
637 filtering schemes. The latter is reflected by differences in spatial coverage (e.g., WFMD methane is
638 not restricted to land observations only) and number of retrievals over a given region (see right hand
639 side panels of Figure 9). The data density differs significantly depending on region. Typically WFMD
640 has many more data points over the Sahara and other areas in the ~10^o-40^oN latitude range but also
641 over mid/northern Australia and the mid/western part of the US, whereas IMAP has higher data

density over South America and mid/high northern latitudes. Large differences between the two data sets are also visible over large parts of northern Africa, where IMAP methane is higher (by approx. 40 ppb) and Greenland, where WFMD methane is higher (by approx. 40 ppb). The reasons for the differences have not yet been identified. It has also not yet been assessed to what extent inferred regional methane fluxes would differ depending on which data set is used as input data for inverse modeling of regional methane fluxes. Significant differences can be expected as the regional differences exceed the bias threshold requirement of less than 10 ppb. The discussion also shows that depending on region the differences can be significantly larger than the estimated biases listed in Table 5, which are based on the analysis of the satellite data at TCCON sites only. Clearly, more research is needed to understand the differences between the two SCIAMACHY methane data sets discussed in this section.

5.5 Inter-comparison of TANSO XCH_4 data products

Within GHG-CCI, four TANSO XCH_4 retrieval algorithms have been further developed and used to generate global data sets which have been inter-compared and compared with TCCON retrievals and global model data (Buchwitz et al., 2012a). The four retrieval algorithms are the FP and PR algorithms developed by SRON (SRFP, SRPR) and Univ. Leicester (UoL; OCFP and OCPR algorithms).

For the PR algorithms, which are based on the retrieval of ratios of the CH_4 to CO_2 columns, followed by a model-based CO_2 correction to compute XCH_4, the column ratios have been compared as well as the final XCH_4 product. As expected, it has been found that the agreement between the ratios is typically somewhat better compared to the XCH_4 products due to differences between the model-based CO_2 correction as used by SRON and UoL (see Buchwitz et al., 2012a, for details). Overall and in line with the discussion presented in Section 5.2, it has been found that the two PR products agree nearly equally well with the TCCON ground-based observations. A direct comparison of the two data products at TCCON sites is also shown in Figure 11 indicating agreement within typically 10 ppb (1-sigma). Nevertheless, inspection of global maps also reveals significant differences, depending on region and time. Qualitatively, this is similar to the results found for the SCIAMACHY data sets discussed in the previous section, but the differences shown in Figure 11 for TANSO are significantly

669 smaller compared to the differences for SCIAMACHY shown in Figures 9 and 10. Figure11 shows a
670 global OCPR-SRPR methane difference map for July 2009. As can be seen, the differences may
671 exceed 5 ppb (breakthrough requirement) or even 10 ppb (threshold requirement) over certain
672 extended regions such as India. Comparisons between the two FP TANSO XCH_4 data products OCFP
673 and SRFP have also been carried out. Using SRFP, two years of global TANSO data have been
674 retrieved but the comparison had to be limited to TCCON sites only because of limitations of the
675 OCFP data set which is not yet available globally. It has been found that the inter-station bias is
676 smaller for SRFP (~4 ppb) compared to OCFP (~8 ppb) and that the scatter of the SRFP data is
677 somewhat smaller compared to the OCFP (14 ppb versus 16 ppb). These findings are consistent with
678 the results presented in Table 5 but have been derived independently (see Buchwitz et al., 2012a). It
679 has also been found that the agreement between the two PR algorithms is significantly better than the
680 agreement between the two FP algorithms. This may be due to the fact that PR algorithms are simpler
681 but may also indicate that at the current stage of development the PR algorithms are more mature (note
682 that they also deliver much more data points, see Section 5.2).

683 **5.6 Algorithm selection results**

684 The main goal of the RR exercise was to determine which satellite retrieval algorithms to use to
685 generate the CRDP. Based on the results presented and discussed in the previous sections, algorithms
686 have been selected. The selection results are presented in the following sub-sections.

687 **5.6.1 Selection results: SCIAMACHY and GOSAT XCO_2**

688 Within GHG-CCI, two SCIAMACHY and two TANSO XCO_2 algorithms have been further
689 developed and the corresponding data products have been inter-compared. They have also been
690 compared with three other TANSO XCO_2 data products generated outside of this project: with the two
691 TANSO XCO_2 products generated at NIES, Japan, (i.e., the operational TANSO product (Yoshida et
692 al., 2011) and the scientific PPDF product (Oshchepkov et al., 2011)) and with the NASA ACOS team
693 product (O'Dell et al., 2012, Crisp et al., 2012). Analysis of all seven products indicates that the
694 precision requirement has been met, but not the very demanding bias requirement of less than 0.5 ppm

(approximately 1 ppm has been achieved at TCCON sites). Clearly, more work on the individual retrieval algorithms is required to achieve this goal and it has been decided to continue with all algorithms. A possible exception is the fast SCIAMACHY XCO_2 WFMD algorithm, which shows a reduced data quality in terms of precision and biases compared to the computationally much more demanding BESD algorithm. On the other hand the WFMD product has significantly (3-4 times) more data points compared to BESD and therefore much better coverage compared to any of the other data products including BESD. GHG-CCI aims at taking advantage of the fact that an ensemble of state-of-the-art data products exists which can be exploited. To this end, the EnseMble Median Algorithm (EMMA) has been developed (Reuter et al., 2013). EMMA generates a Level 2 XCO_2 product using the median of the individual data products thereby largely eliminating outliers of the data products generated with the individual algorithms. EMMA may also improve the error characterization using the ensemble scatter. Preliminary analysis indicates that EMMA outperforms each of the individual algorithms. EMMA also permits the identification of potential weaknesses of the individual algorithms, which can be used to improve the individual algorithms. Taking this into account, it has been decided to proceed with all satellite XCO_2 algorithms and to add the EMMA data product to the GHG-CCI product portfolio.

5.6.2 Selection results: SCIAMACHY XCH_4

Data products generated with two algorithms have been assessed: WFMD (Schneising et al., 2011, 2012) and IMAP (Frankenberg et al., 2011). Comparison with ground-based TCCON observations revealed that both data products are very similar with respect to biases. This is also true for the estimated single measurement precisions for the time period 2003-2005, when the SCIAMACHY detector did not yet suffer from major degradation in the spectral region needed for methane retrieval.

After 2005, the WFMD methane shows a larger scatter (~80 ppb) compared to IMAP (~50 ppb). Both data products have to be used with care for the time after 2005 due to potential bias issues related to detector degradation as indicated by the TCCON comparison at southern hemisphere TCCON sites, where both data products show a low bias of 20-30 ppb depending on FTS site. Considering only this

analysis, one would conclude that both data products are essentially equivalent and one may therefore select one of them. Analysis of spatially resolved global methane distributions as generated by the two algorithms however shows significant differences, depending on region and time, which are larger than the required maximum bias of 10 ppb, i.e., are significant for regional-scale methane surface flux inversions. Due to the lack of appropriate reference data such as TCCON, it was not yet possible to determine which of the two data products is the most accurate. Therefore, it has been decided to proceed with both algorithms and to contribute with both alternative data products to the CRDP pointing out the strength and weaknesses of the two approaches. Users will be encouraged to use both data sets, to determine to what extent their findings depend on the data product used, and to report these findings to the GHG-CCI retrieval experts.

5.6.3 Selection results: TANSO XCH_4

Four algorithms and their corresponding data products have been evaluated: OCFP and OCPR (Parker et al., 2011) and SRFP and SRPR (Butz et al., 2011). All data products show very similar biases and scatter when compared with ground-based TCCON observations. The number of data points is however significantly higher for the "Proxy" (PR) algorithms compared to the "Full Physics" (FP) algorithms and the agreement between the two PR data products is better than for the FP products, indicating a higher level of maturity of the (simpler) PR algorithms. Note that the SCIAMACHY XCH_4 algorithms, WFMD and IMAP, are also PR algorithms and that the FP algorithms are relatively new and currently in their early stages of development. Overall, the OCPR algorithm shows a slightly better performance compared to SRPR (primarily in terms of number of data points at TCCON sites). It has therefore been decided to continue with OCPR within GHG-CCI. The PR XCH_4 algorithms depend on a CO_2 correction using model data. The long-term goal of GHG-CCI is to use a FP algorithm that is independent of a CO_2 model. Because the SRFP algorithm shows a somewhat better performance compared to the OCFP algorithm (e.g., lower station-to-station biases at TCCON sites), it has been decided to continue with the SRFP algorithm, despite the lower number of data points compared to OCFP. In summary, four TANSO XCH_4 algorithms have been evaluated as part of

747 the GHG-CCI RR and two of these algorithms have been selected for further use within GHG-CCI:
748 OCPR and SRFP.

749 **6. Additional Constraints Algorithms (ACAs)**

750 The Additional Constraints Algorithms (ACAs) are algorithms to retrieve CO_2 and/or CH_4 information
751 for layers above the planetary boundary layer. ACAs are applied to several satellite instruments. An
752 overview of the ACAs used within GHG-CCI is given in Table 3. As the ACAs are not the focus of
753 this manuscript the reader is referred to the references listed in Table 3 (including caption) for details
754 on each of these algorithms and corresponding data products.

755 For ACAs only one algorithm per data product has been considered within GHG-CCI, i.e., ACAs are
756 also being further developed but not in competition and not by covering all aspects (e.g., no dedicated
757 validation). For ACAs a number of criteria have been defined which need to be fulfilled to contribute
758 to the CRDP but detailed user requirements have not been formulated.

759 Only a limited assessment of the data products generated with ACAs has been conducted during the
760 initial phase of GHG-CCI described in this manuscript because the focus was on ECAs. However, for
761 each of the ACAs listed in Table 3 it has been determined if the selection criteria specified in the
762 Round Robin Evaluation Procedure (RREP, Buchwitz et al., 2011b) have been met. The RREP defines
763 11 criteria for ACAs which need to be fulfilled for a given ACA to contribute to the CRDP. The
764 criteria are mostly qualitative and refer to a required minimum level of documentation, error analysis
765 and related auxiliary information. All ACA products are potentially useful for GHG-CCI climate
766 applications as they deliver additional information on CO_2 and/or CH_4 thereby providing potentially
767 important constraints when used, for example, within an appropriate inverse modeling framework to
768 derive regional surface fluxes from the satellite observations. However, no detailed user requirements
769 are currently available, no dedicated validation has been performed within GHG-CCI and it has also
770 not been assessed to what extent the existing products are useful or not useful for GHG surface flux
771 inverse modeling. More research is needed to assess the usefulness of these data products for climate

relevant applications. It has been identified that all ACAs fulfill the requirements listed in the RREP and that all ACA products can therefore be included in the CRDP.

7. Climate Research Data Package (CRDP)

The goal of the GHG-CCI RR was to decide which algorithms to use to generate the CRDP. It is planned to generate the CRDP during September 2012 to March 2013. Table 6 presents an overview of the planned content of the CRDP in terms of data products and their spatio-temporal coverage. The CRDP will contain all relevant information needed for inverse modeling such as single observation uncertainties, *a priori* profiles and averaging kernels. The CRDP will be validated during March-May 2013 and subsequently evaluated by the GHG-CCI users (June-August 2013). By the end of August, the CRDP along with the corresponding documentation will be made publicly available via the GHG-CCI website.

8. Summary and conclusions

An overview of the main activities and results achieved during the first two years of the GHG-CCI project of ESA's Climate Change Initiative (CCI) has been presented, focusing on the CCI "Round Robin" (RR) exercise. The goal of CCI is to generate a number of Essential Climate Variables (ECVs) in-line with GCOS (Global Climate Observing System) requirements and guidelines using European Earth observation data and data from ESA Third Party Missions (TPM) such as GOSAT. To achieve this, several existing state-of-the-art retrieval algorithms for retrieving XCO_2 and XCH_4 from SCIAMACHY/ENVISAT and TANSO/GOSAT nadir radiance spectra have been further improved in order to meet challenging requirements for the targeted regional CO_2 and CH_4 surface flux (source/sink) application as defined by the GHG-CCI Climate Research Group (CRG). The ultimate goal of the RR was to identify and select the best algorithms to be used for generating the Climate Research Data Package (CRDP), which will essentially be the first version of the CCI ECV GHG data base. In addition, retrieval algorithms for a number of other satellite instruments such as IASI and MIPAS have also been further developed, but not in competition.

797 Substantial progress has been made during the first two years (September 2010 – August 2012) of the
798 GHG-CCI project. For example, longer XCO_2 and XCH_4 time series have been generated from
799 SCIAMACHY with improved data quality and better error characterization (Reuter et al., 2011,
800 Frankenberg et al., 2011, Schneising et al., 2011, 2012, Heymann et al., 2012a, 2012b). The same is
801 true for TANSO (Butz et al., 2011, Parker et al., 2011, Schepers et al., 2012, Cogan et al., 2012).

802 Several retrieval algorithms have been further developed in competition during the GHG-CCI RR and
803 used to generate global multi-year data sets of XCO_2 and XCH_4 from SCIAMACHY and TANSO.
804 The data products have been evaluated by comparison with ground-based TCCON observations, by
805 inter-comparisons of the data products generated with the different candidate algorithms, and by
806 comparisons with other data sets including global models. Due to the sparseness of the TCCON
807 network it was not planned to base the algorithm selection decision only on satellite – TCCON
808 comparisons. It has been found that nearly all candidate algorithms produce data with very similar
809 quality at TCCON sites, i.e., show similar satellite – TCCON differences. Significant differences have
810 however been found remote from TCCON when comparing the global data sets, e.g., when comparing
811 global maps. Depending on region and time, it has been found that the differences may exceed the
812 systematic error requirements of less than 0.5 ppm for XCO_2 and 10 ppb for XCH_4. It has been
813 identified that more research is needed in order to understand the differences between the various data
814 sets. It was therefore not possible for all products to clearly identify which of the candidate algorithms
815 performs best. The goal of the RR was to identify which of the competing algorithms to use for the
816 CRDP. The selected algorithms are listed in Table 6. A summary of the RR algorithm selection
817 decision and justification is given in Section 5.6 for the GHG-CCI ECV core data products and in
818 Section 6 for additional products generated with algorithms not in competition during the RR phase.

819 The climate and inverse modeling community requires long-term datasets of near-surface-sensitive
820 CO_2 and CH_4 observations that are as accurate and precise as possible. The goal of GHG-CCI is to
821 build up such a time series starting with SCIAMACHY/ENVISAT (March 2002 – April 2012) and
822 being continued with GOSAT (launch 2009) and future GHG satellite missions such as OCO-2
823 (Boesch et al., 2011), Sentinel-5-Precursor (Butz et al., 2012) and potentially CarbonSat

(Bovensmann et al., 2010). As shown in this manuscript, significant progress has been made to achieve this goal, but more work is needed in order to meet the demanding user requirements for as many conditions as possible.

9. Acknowledgements

This work was primarily funded by ESA/ESRIN (GHG-CCI) but also received funding from EU FP7 (grant agreement No. 283576, MACC-II), DLR (SADOS), and the State and the University of Bremen. We thank the members of the GOSAT Project (JAXA, NIES, and Ministry of the Environment (MoE), Japan) for providing GOSAT Level 1B and Level 2 data products (GOSAT RA1 PI project CONSCIGO). The ACOS v2.9 data were produced by the ACOS/OCO-2 project at the Jet Propulsion Laboratory, California Institute of Technology, and obtained from the ACOS/OCO-2 data archive maintained at the NASA Goddard Earth Science Data and Information Services Center. We thank NOAA for making available the CarbonTracker CO_2 fields. We also thank TCCON and related funding organizations (NASA grants NNX11AG01G, NAG5-12247, NNG05-GD07G, NASA Orbiting Carbon Observatory Program, DOE ARM program, the Australian Research Council, DP0879468 and LP0562346, the EU projects IMECC and GEOmon, the Senate of Bremen). Last but not least we would like to thank the two referees for helpful comments.

841

842 **10. References**

843 Bergamaschi, P., Frankenberg, C., Meirink, J.F., Krol, M., Dentener, F., Wagner, T., Platt, U., Kaplan,
844 J.O., Körner, S., Heimann, M., Dlugokencky, E.J., Goede, A. (2007), Satellite chartography of
845 atmospheric methane from SCIAMACHY onboard ENVISAT: 2. Evaluation based on inverse
846 model simulations, *J. Geophys. Res*., 112, D02304, doi:10.1029/2006JD007268.

847 Bergamaschi, P., Frankenberg, C., Meirink, J. F., Krol, M., Villani, M. G., Houweling, S., Dentener,
848 F., Dlugokencky, E. J., Miller, J. B., Gatti, L. V., Engel, A., Levin, I. (2009), Inverse modeling
849 of global and regional CH_4 emissions using SCIAMACHY satellite retrievals, J. *Geophys.*
850 *Res.,* 114, D22301, doi:10.1029/2009JD01228.

851 Bloom, A. A., Palmer, P. I., Fraser, A., Reay, D. S., Frankenberg, C. (2010), Large-scale controls of
852 methanogenesis inferred from methane and gravity spaceborne data, Science, 327, 322–325,
853 doi:10.1126/science.1175176.

854 Boesch, H., Baker, D., Connor, B., Crisp, D., Miller, C. (2011): Global Characterization of CO_2
855 Column Retrievals from Shortwave-Infrared Satellite Observations of the Orbiting Carbon
856 Observatory-2 Mission, Remote Sens., 3, 270–304, doi:10.3390/rs3020270,
857 http://www.mdpi.com/2072-4292/3/2/270/ .

858 Bovensmann, H., Burrows, J. P., Buchwitz, M., Frerick, J., Noël, S., Rozanov, V. V., Chance, K. V.,
859 Goede, A. H. P. (1999), SCIAMACHY - Mission objectives and measurement modes, *J.*
860 *Atmos. Sci.*, 56 (2), 127-150.

861 Bovensmann, H., Buchwitz, M., Burrows, J. P., Reuter, M., Krings, T., Gerilowski, K., Schneising, O.,
862 Heymann, J., Tretner, A., Erzinger, J. (2010), A remote sensing technique for global
863 monitoring of power plant CO_2 emissions from space and related applications, *Atmos. Meas.*
864 *Tech*., 3, 781-811.

865 Bril, A., Oshchepkov, S., Yokota, T., Inoue, G. (2007): Parameterization of aerosol and cirrus cloud
866 effects on reflected sunlight spectra measured from space: application of the equivalence
867 theorem, *Appl. Opt.*, Vol.46(13), 2460-2470.

868 Buchwitz, M., Rozanov, V. V., Burrows, J. P. (2000), A near-infrared optimized DOAS method for
869 the fast global retrieval of atmospheric CH_4, CO, CO_2, H_2O, and N_2O total column amounts
870 from SCIAMACHY Envisat-1 nadir radiances, *J. Geophys. Res.*, 105, 15,231-15,245.

871 Buchwitz, M., de Beek, R., Burrows, J. P., Bovensmann, H., Warneke, T., Notholt, J., Meirink, J. F.,
872 Goede, A. P. H., Bergamaschi, P., Körner, S., Heimann, M., Schulz, A. (2005), Atmospheric
873 methane and carbon dioxide from SCIAMACHY satellite data: Initial comparison with
874 chemistry and transport models, *Atmos. Chem. Phys*., 5, 941-962.

875 Buchwitz, M., Schneising, O., Burrows, J. P., Bovensmann, H., Reuter, M., Notholt, J. (2007), First
876 direct observation of the atmospheric CO_2 year-to-year increase from space, *Atmos. Chem.*
877 *Phys*., 7, 4249-4256.

878 Buchwitz, M., Chevallier, F., Bergamaschi, P. (2011a), User Requirements Document (URD) for the
879 GHG-CCI project of ESA's Climate Change Initiative, Technical Report, pp. 45, version 1
880 (URDv1), 3. February 2011, available from http://www.esa-ghg-cci.org.

881 Buchwitz, M., Reuter, M., Chevallier, F., Bergamaschi, P. (2011b), Round Robin Evaluation Protocol
882 (RREP) for the GHG-CCI project of ESA's Climate Change Initiative, Technical Report, pp.
883 15, version 2 (RREPv2), 17. August 2011, available from http://www.esa-ghg-cci.org.

884 Buchwitz, M., Reuter, M., Schneising, O., Parker, R., Guerlet, Noël, S., S. Crevoisier, C., Laeng, A.
885 (2011c), Algorithm Inter-comparison and Error Characterization & Analysis Report
886 (AIECAR) of the GHG-CCI project of ESA's Climate Change Initiative, Technical Report,
887 pp. 192, version 0 (AIECARv0), 22. August 2011, available from http://www.esa-ghg-cci.org.

888 Buchwitz, M., Reuter, M., Schneising, O., Parker, R., Guerlet, Noël, S., S. Crevoisier, C., Laeng, A.
889 (2012a), Algorithm Inter-comparison and Error Characterization & Analysis Report

(AIECAR) of the GHG-CCI project of ESA's Climate Change Initiative, Technical Report, version 1 (AIECARv1), 28. August 2012, available from http://www.esa-ghg-cci.org.

Buchwitz, M., Chevallier, F., Bergamaschi, P., Kaminski, T. (2012b), Algorithm Selection Report (ASR) of the GHG-CCI project of ESA's Climate Change Initiative, Technical Report, 29. August 2012, available from http://www.esa-ghg-cci.org.

Butz, A., Guerlet, S., Hasekamp, O., Schepers, D., Galli, A., Aben, I., Frankenberg, C., Hartmann, J.-M., Tran, H., Kuze, A., Keppel-Aleks, G., Toon, G., Wunch, D., Wennberg, P., Deutscher, N., Griffith, D., Macatangay, R. , Messerschmidt, J., Notholt, J. , Warneke, T. (2011), Towards accurate CO_2 and CH_4 observations from GOSAT, *Geophys. Res. Lett.*, doi:10.1029/2011GL047888.

Butz, A., Galli, A., Hasekamp, O., Landgraf, J., Tol, J. P., Aben, I. (2012), TROPOMI aboard Sentinel-5 Precursor: Prospective performance of CH_4 retrievals for aerosol and cirrus loaded atmospheres, *Remote Sensing of Environment*, 120, 267 – 276.

Canadell, J. G., Ciais, P., Dhakal, S., Dolman, H., Friedlingstein, P., Gurney. K. R,, Held, A., Jackson, R. B., Le Quéré, C., Malone, E. L., Ojima, D. S., Patwardhan, A., Peters, G. P., Raupach, M. R. (2010), Interactions of the carbon cycle, human activity, and the climate system: a research portfolio, *Current Opinion in Environmental Sustainability*, 2, 301–311, available online at www.sciencedirect.com.

Chevallier, F., Engelen, R. J., Peylin, P. (2005), The contribution of AIRS data to the estimation of CO_2 sources and sinks. *Geophys. Res. Lett.*, 32, L23801, doi:10.1029/ 2005GL024229.

Chevallier, F., Bréon, F.-M., and Rayner, P. J. (2007), Contribution of the Orbiting Carbon Observatory to the estimation of CO_2 sources and sinks: Theoretical study in a variational data assimilation framework, *J. Geophys. Res*., 112, D09307, doi:10.1029/2006JD007375.

Cogan, A., Boesch, H., Parker, R., Feng, L., Palmer, P., Blavier, J.-F., Deutscher, N., Macatangay, R., Notholt, J., Roehl, C. M., Warneke, T., Wunch, D. (2012), Atmospheric carbon dioxide retrieved from the Greenhouse gases Observing SATellite: Comparison with ground-based

916 TCCON observations and GEOS-Chem model calculations*, J. Geophys. Res.*, 117, D21,
917 doi:10.1029/2012JD018087.

918 Crevoisier, C., Heilliette, S., Chédin, A., Serrar, S., Armante, R., Scott, N.A. (2004), Midtropospheric
919 CO_2 concentration retrieval from AIRS observations in the tropics, *Geophys. Res. Lett.*, 31,
920 L17106, doi:10.1029/2004GL020141.

921 Crevoisier, C., Chédin, A., Matsueda, H., Machida, T., Armante, R., Scott, N. A. (2009a), First year of
922 upper tropospheric integrated content of CO_2 from IASI hyperspectral infrared observations,
923 *Atmos. Chem. Phys.*, 9, 4797–4810.

924 Crevoisier, C., Nobileau, D., Fiore, A., Armante, R., Chédin, A., Scott, N. A. (2009b), Tropospheric
925 methane in the tropics – first year from IASI hyperspectral infrared observations, *Atmos.*
926 *Chem. Phys.*, 9, 6337–6350.

927 Crisp, D., Atlas, R. M., Bréon, F.-M., Brown, L. R., Burrows, J. P., Ciais, P., Connor, B. J., Doney, S.
928 C., Fung, I. Y., Jacob, D. J., Miller, C. E., O'Brien, D., Pawson, S., Randerson, J. T., Rayner,
929 P., Salawitch, R. S., Sander, S. P., Sen, B., Stephens, G. L., Tans, P. P., Toon, G. C.,
930 Wennberg, P. O., Wofsy, S. C., Yung, Y. L., Kuang, Z., Chudasama, B., Sprague, G., Weiss,
931 P., Pollock, R., Kenyon, D., Schroll, S. (2004), The Orbiting Carbon Observatory (OCO)
932 mission, *Adv. Space Res.*, 34, 700-709.

933 Crisp, D., Fisher, B. M., O'Dell, C., Frankenberg, C., Basilio, R., Boesch, H. L. R. Brown, R.
934 Castano, B. Connor, N. M. Deutscher, A. Eldering, D. Griffith, M. Gunson, A. Kuze, L.
935 Mandrake, J. McDuffie, J. Messerschmidt, C. E. Miller, I. Morino, V. Natraj, J. Notholt, D. M.
936 O'Brien, F. Oyafuso, I. Polonsky, J. Robinson, R. Salawitch, V. Sherlock, M. Smyth, H. Suto,
937 T. E. Taylor, D. R. Thompson, P. O.Wennberg, D.Wunch, Y. L. Yung (2012), The ACOS CO_2
938 retrieval algorithm – Part II: Global XCO_2 data characterization, *Atmos. Meas. Tech.*, 5, 687–
939 707.

940 Deutscher, N. M., Griffith, D. W. T., Bryant, G. W., Wennberg, P. O., Toon, G. C., Washenfelder, R.
941 A., Keppel-Aleks, G., Wunch, D., Yavin, Y. G., Allen, N. T., Blavier, J.-F. L., Jiménez, R.,

Daube, B. C., Bright, A. V, Matross, D. M., Wofsy, S. C., Park, S. (2010), Total column CO_2 measurements at Darwin, Australia – site description and calibration against in situ aircraft profiles, *Atmos. Meas. Tech.*, 3(4), 947–958, doi:10.5194/amt-3-947-2010.

Dlugokencky, E. J., Bruhwiler, L., White, J. W. C., Emmons, L. K., Novelli, P. C., Montzka, S. A., Masarie, K. A., Lang, P. M., Crotwell, A. M., Miller, J. B., Gatti, L. V. (2009), Observational constraints on recent increases in the atmospheric CH_4 burden, *Geophys. Res. Lett.*, 36, L18803, doi:10.1029/2009GL039780.

Sussmann, R., Ostler, A., Forster, F., Rettinger, M., Deutscher, N. M., Griffith, D. W. T., Hannigan, J. W., Jones, N., Patra, P. K. (2013), First intercalibration of column-averaged methane from the Total Carbon Column Observing Network and the Network for the Detection of Atmospheric Composition Change, *Atmos. Meas. Tech.*, 6, 397–418.

Foucher, P. Y., Chédin, A., Dufour, G., Capelle, V., Boone, C. D., Bernath, P. (2009), Technical Note: Feasibility of CO_2 profile retrieval from limb viewing solar occultation made by the ACE-FTS instrument, *Atmos. Chem. Phys*., 9, 2873–2890.

Frankenberg, C., Meirink, J. F., van Weele, M., Platt, U., Wagner, T. (2005), Assessing methane emissions from global spaceborne observations, *Science*, 308, 1010–1014.

Frankenberg, C., Aben, I., Bergamaschi, P., Dlugokencky, E. J., van Hees, R., Houweling, S., van der Meer, P., Snel, R., Tol, P. (2011), Global column-averaged methane mixing ratios from 2003 to 2009 as derived from SCIAMACHY: Trends and variability, *J. Geophys. Res*., doi:10.1029/2010JD014849.

GCOS (Global Climate Observing System) (2006), Systematic Observation Requirements for Satellite-based products for Climate – Supplemental Details to the GCOS Implementation Plan, GCOS 107, September 2006.

Geibel, M. C., Messerschmidt, J., Gerbig, C., Blumenstock, T., Chen, H., Hase, F., Kolle, O., Lavric, J. V., Notholt, J., Palm, M., Rettinger, M., Schmidt, M., Sussmann, R., Warneke, T., Feist, D. G. (2012), Calibration of column-averaged CH_4 over European TCCON FTS sites with

968 airborne in-situ measurements, *Atmos. Chem. Phys.*, 12, 8763–8775, doi:10.5194/acp-12-
969 8763-2012.

970 Heymann, J., Schneising, O., Reuter, M., Buchwitz, M., Rozanov, V. V., Velazco, V. A.,
971 Bovensmann, H., Burrows, J. P. (2012a), SCIAMACHY WFM-DOAS XCO_2: comparison
972 with CarbonTracker XCO_2 focusing on aerosols and thin clouds, *Atmos. Meas. Tech.*, 5, 1935-
973 1952, 2012.

974 Heymann, J., Bovensmann, H., Buchwitz, M., Burrows, J. P., Deutscher, N. M., Notholt, J., Rettinger,
975 M., Reuter, M., Schneising, O., Sussmann, R., Warneke. T. (2012b), SCIAMACHY WFM-
976 DOAS XCO_2: reduction of scattering related errors, *Atmos. Meas. Tech.*, 5, 2375-2390, 2012.

977 Kaminski, T., Scholze, M., Houweling, S. (2010), Quantifying the Benefit of A-SCOPE
978 Data for Reducing Uncertainties in Terrestrial Carbon Fluxes in CCDAS. *Tellus B*,
979 doi:10.1111/j.1600-0889.2010.00483.x

980 Kaminski, T., Knorr, W., Scholze, M., Gobron, N., Pinty, R., Giering, R., Mathieu, P.-P. (2012),
981 Consistent Assimilation of MERIS FAPAR and atmospheric CO_2 into a Terrestrial Vegetation
982 Model and Interactive Mission Benefit Analysis. *Biogeosciences*, 9(8):3173-3184.

983 Knutti, R., R. Furrer, C. Tebaldi, J. Cermak, G. A. Meehl (2010), Challenges in Combining
984 Projections from Multiple Climate Models. *J. Climate*, 23, 2739–2758. doi:
985 http://dx.doi.org/10.1175/2009JCLI3361.1

986 Kuze, A., Suto, H., Nakajima, M., and Hamazaki, T. (2009), Thermal and near infrared sensor for
987 carbon observation Fourier-transform spectrometer on the Greenhouse Gases Observing
988 Satellite for greenhouse gases monitoring, *Appl. Opt*., 48, 6716–6733.

989 Meirink, J. F., Eskes, H. J., and Goede, A. P. H. (2006), Sensitivity analysis of methane emissions
990 derived from SCIAMACHY observations through inverse modelling, *Atmos. Chem. Phys*., 6,
991 1275–1292.

992 Messerschmidt, J., Geibel, M. C., Blumenstock, T., Chen, H., Deutscher, N. M., Engel, A., Feist, D.
993 G., Gerbig, C., Gisi, Hase, M. F., Katrynski, K., Kolle, O., Lavric, J. V., Notholt, J., Palm, M.,

994 Ramonet, M., Rettinger, M., Schmidt, M., Sussmann, R., Toon, G. C., F. Truong, F., Warneke,
995 T., Wennberg, P. O., Wunch, D., Xueref-Remy, I. (2012), Calibration of TCCON column-
996 averaged CO_2: the first aircraft campaign over European TCCON sites, *Atmos. Chem. Phys*.,
997 11, 10765-10777.

998 Noël, S., Bramstedt, K., Rozanov, A., Bovensmann, H., Burrows, J. P. (2011), Stratospheric methane
999 profiles from SCIAMACHY solar occultation measurements derived with onion peeling
1000 DOAS, *Atmos. Meas. Tech*., 4, 2567-2577.

1001 Notholt, J., Dils, B., Blumenstock,T., Brunner, D., Buchmann, B., De Mazière, M., Popp, C.,
1002 Sussmann, R. (2012), Product Validation and Algorithm Selection Report (PVASR) of the
1003 GHG-CCI project of ESA's Climate Change Initiative, Technical Report, 22. August 2012,
1004 available from http://www.esa-ghg-cci.org.

1005 O'Dell, C. W., Connor, B., Boesch, H., O'Brien, D., Frankenberg, C., Castano, R., Christi, M.,
1006 Eldering, D., Fisher, B., Gunson, M., McDuffie, J., Miller, C. E., Natraj, V., Oyafuso, F.,
1007 Polonsky, I., Smyth, M., Taylor, T., Toon, G. C., Wennberg, P. O., Wunch, D., (2012), The
1008 ACOS CO_2 retrieval algorithm – Part 1: Description and validation against synthetic
1009 observations, *Atmos. Meas. Tech*., 5, 99–121, 2012.

1010 Oshchepkov S., Bril, A., Yokota, T. (2008), PPDF-based method to account for atmospheric light
1011 scattering in observations of carbon dioxide from space. J. Geophys. Res., 113, D23210.

1012 Oshchepkov S., Bril, A., Yokota, T. (2009), An improved photon path length probability density
1013 function-based radiative transfer model for space-based observation of greenhouse gases. *J.*
1014 *Geophys. Res.*, 114, D19207.

1015 Oshchepkov, S., Bril, A., Maksyutov, S., Yokota, T. (2011), Detection of optical path in spectroscopic
1016 space-based observations of greenhouse gases: Application to GOSAT data processing, *J.*
1017 *Geophys. Res*., 116, D14304, doi:10.1029/2010JD015352.

1018 Oshchepkov, S., Bril, A., Yokota, T., Morino, I., Yoshida, Y., Matsunaga, T., Belikov, D., Wunch, D.,
1019 Wennberg, P., Toon, G., O'Dell, C., Butz, A., Guerlet, S., Cogan, A., Boesch, H., Eguchi, N.,
1020 Deutscher, N., Griffith, G., Macatangay, R., Notholt, J., Sussmann, R., Rettinger, M.,

1021 Sherlock, V., Robinson, J., Kyrö, E., Heikkinen, P., Feist, D. G., Nagahama,T., Kadygrov, N.,
1022 Maksyutov, S., Uchino, O., Watanabe, H. (2012), Effects of atmospheric light scattering on
1023 spectroscopic observations of greenhouse gases from space: Validation of PPDF-based CO_2
1024 retrievals from GOSAT, J. Geophys. Res., 117, D12305, doi:10.1029/2012JD017505.
1025 Parker, R., Boesch, H., Cogan, A., Fraser, A., Feng, L, Palmer, P., Messerschmidt, J., Deutscher, N.,
1026 Griffth, D., Notholt, J., Wennberg, P. Wunch, D. (2011), Methane Observations from the
1027 Greenhouse gases Observing SATellite: Comparison to ground-based TCCON data and Model
1028 Calculations, *Geophys. Res. Lett*., doi:10.1029/2011GL047871.
1029 Peters, W., Jacobson, A. R., Sweeney, C., Andrews, A. E., Conway, T. J., Masarie, K., Miller, J. B.,
1030 Bruhwiler, L. M. P., Petron, G., Hirsch, A. I., Worthy, D. E. J., van der Werf, G. R.,
1031 Randerson, J. T., Wennberg, P. O., Krol, M. C., Tans, P. P. (2007): An atmospheric
1032 perspective on North American carbon dioxide exchange: CarbonTracker, Proceedings of the
1033 National Academy of Sciences (*PNAS*) of the United States of America, 27 Nov. 2007,
1034 104(48), 18925-18930.
1035 Reuter, M., Buchwitz, M., Schneising, O., Heymann, J., Bovensmann, H., Burrows, J. P. (2010), A
1036 method for improved SCIAMACHY CO_2 retrieval in the presence of optically thin clouds,
1037 *Atmos. Meas. Tech*., 3, 209-232.
1038 Reuter, M., Bovensmann, H., Buchwitz, M., Burrows, J. P., Connor, B. J., Deutscher, N. M., Griffith,
1039 D. W. T., Heymann, J., Keppel-Aleks, G., Messerschmidt, J., Notholt, J., Petri, C., Robinson,
1040 J., Schneising, O., Sherlock, V., Velazco, V., Warneke, T., Wennberg, P. O., Wunch, D.
1041 (2011), Retrieval of atmospheric CO_2 with enhanced accuracy and precision from
1042 SCIAMACHY: Validation with FTS measurements and comparison with model results, *J.*
1043 *Geophys. Res*., 116, D04301, doi:10.1029/2010JD015047.
1044 Reuter, M., Schneising, O., Parker, R., Guerlet, S., Noël , S., Crevoisier, C., Laeng, A. (2012a),
1045 Algorithm Theoretical Basis Document (ATBD) of the GHG-CCI project of ESA's Climate
1046 Change Initiative, Technical Report, pp. 486, version 1 (ATBDv1), 15. March 2012, available
1047 from http://www.esa-ghg-cci.org.

1048 Reuter, M., Buchwitz, M., Schneising, O., Hase, F., Heymann, J., Guerlet, S., Cogan, A. J.,
1049 Bovensmann, H., Burrows, J. P., (2012b), A simple empirical model estimating atmospheric
1050 CO_2 background concentrations, *Atmos. Meas. Tech*., 5, 1349-1357.
1051 Reuter, M., Boesch, H., Bovensmann, H., Bril, A., Buchwitz, M., Butz, A., Burrows, J. P., O'Dell, C.
1052 W., Guerlet, S., Hasekamp, O., Heymann, J., Kikuchi, S. Oshchepkov, S., Parker, R., Pfeifer,
1053 S., Schneising, O., Yokota, T., Yoshida, Y. (2013), A joint effort to deliver satellite retrieved
1054 atmospheric CO_2 concentrations for surface flux inversions: The ensemble median algorithm
1055 EMMA, *Atmos. Chem. Phys.*, 13, 1771-1780.
1056 Rigby, M., Prinn, R. G., Fraser, P. J., Simmonds, P. G., Langenfelds, R. L., Huang, J., Cunnold, D. M.,
1057 Steele, L. P., Krummel, P. B., Weiss, R. F., O'Doherty, S., Salameh, P. K., Wang, H. J., Harth,
1058 C. M., Mühle, J., Porter, L. W. (2008), Renewed growth of atmospheric methane, *Geophys.*
1059 *Res. Lett*., 35, L22805, doi:10.1029/2008GL036037.
1060 Rodgers, C. D. (2000), Inverse Methods for Atmospheric Sounding: Theory and Practice, *World*
1061 *Scientific Publishing*.
1062 Schepers, D., Guerlet, S., Butz, A., Landgraf, J., Frankenberg, C., Hasekamp, O., Blavier, J.-F.,
1063 Deutscher, N. M., Griffith, D. W. T., Hase, F., Kyro, E., Morino, I., Sherlock, V., Sussmann,
1064 R., Aben, I. (2012), Methane retrievals from Greenhouse Gases Observing Satellite (GOSAT)
1065 shortwave infrared measurements: Performance comparison of proxy and physics retrieval
1066 algorithms, *J. Geophys. Res*., 117, D10307, doi:10.1029/2012JD017549.
1067 Schneising, O., Buchwitz, M., Burrows, J. P., Bovensmann, H., Reuter, M., Notholt, J., Macatangay,
1068 R., Warneke, T. (2008), Three years of greenhouse gas column-averaged dry air mole
1069 fractions retrieved from satellite - Part 1: Carbon dioxide, *Atmos. Chem. Phys*., 8, 3827-3853,
1070 2008.
1071 Schneising, O., Buchwitz, M., Burrows, J. P., Bovensmann, H., Bergamaschi, P., Peters, W. (2009),
1072 Three years of greenhouse gas column-averaged dry air mole fractions retrieved from satellite
1073 - Part 2: Methane, *Atmos. Chem. Phys*., 9, 443-465.

1074 Schneising, O., Buchwitz, M., Reuter, M., Heymann, J., Bovensmann, H., and Burrows, J. P. (2011),
1075 Long-term analysis of carbon dioxide and methane column-averaged mole fractions retrieved
1076 from SCIAMACHY, *Atmos. Chem. Phys*., 11, 2881-2892.
1077 Schneising, O., Bergamaschi, P., Bovensmann, H., Buchwitz, M., Burrows, J. P., Deutscher, N. M.,
1078 Griffith, D. W. T., Heymann, J., Macatangay, R., Messerschmidt, J., Notholt, J., Rettinger, M.,
1079 Reuter, M., Sussmann, R., Velazco, V. A., Warneke, T., Wennberg, P. O., Wunch, D. (2012),
1080 Atmospheric greenhouse gases retrieved from SCIAMACHY: comparison to ground-based
1081 FTS measurements and model results, *Atmos. Chem. Phys*., 12, 1527-1540.
1082 Simpson, I. J., Sulbaek Andersen, M. P., Meinardi, S., Bruhwiler, L., Blake, N. J., Helmig, D.,
1083 Rowland, F. S., Blake, D. R. (2012), Long-term decline of global atmospheric ethane concentrations
1084 and implications for methane, *Nature*, www.nature.com/doifinder/10.1038/nature11342
1085 Solomon, S., Qin, D., Manning, M., Chen, Z., Marquis, M., Averyt, K. B., Tignor, M., and Miller, H.
1086 L. (Eds.): Climate Change 2007: The Physical Science Basis, Contribution of Working Group
1087 I to the Fourth Assessment Report of the Intergovernmental Panel on Climate Change (IPCC),
1088 *Cambridge University Press*, Cambridge, United Kingdom and New York, NY, USA, 2007.
1089 Stephens, B. B., Gurney, K. R., Tans, P. P., Sweeney, C., Peters, W., Bruhwiler, L., Ciais, P.,
1090 Ramonet, M., Bousquet, P., Nakazawa, T., Aoki, S., Machida, T., Inoue, G., Vinnichenko, N.,
1091 Lloyd, J., Jordan, A., Heimann, M., Shibistova, O., Langenfelds, R. L., Steele, L. P., Francey,
1092 R. J., and Denning, A. S. (2007), Weak northern and strong tropical land carbon uptake from
1093 vertical profiles of atmospheric CO_2, *Science*, 316, 1732–1735.
1094 Toon, G. (1991), The JPL MkIV interferometer, *Optics Photonics News*, 2, 19–21.
1095 von Clarmann, T., Höpfner, M., Kellmann, S., Linden, A., Chauhan, S., Funke, B., Grabowski, U.,
1096 Glatthor, N., Kiefer, M., Schieferdecker, T., Stiller, G., Versick, S. (2009), Retrieval of
1097 temperature, H_2O, O_3, HNO_3, CH_4, N_2O, $ClONO_2$ and ClO from MIPAS reduced resolution
1098 nominal mode limb emission measurements, *Atmos. Meas. Tech*., 2, 159-175.
1099 Wecht, K. J., Jacob, D. J., Wofsy, S. C., Kort, E. A., Worden, J. R., Kulawik, S. S., Henze, D. K., M.
1100 Kopacz, M., H. Payne, V. H. (2012), Validation of TES methane with HIPPO aircraft

observations: implications for inverse modeling of methane sources, *Atmos. Chem. Phys*., 12, 1823–1832.

Wofsy, S. C., Daube, B. C., Jimenez, R., Kort, E., Pittman, J. V., Park, S., Commane, R., Xiang, B., Santoni, G., Jacob, D., Fisher, J., Pickett-Heaps, C., Wang, H., Wecht, K., Wang, Q.-Q., Stephens, B. B., Schertz, S., Romashkin, P., Campos, T., Haggerty, J., Cooper, W. A., Rogers, D., Beaton, S., Elkins, J. W., Fahey, D., Gao, R., Moore, F., Montzka, S. A., Schwartz, J. P., Hurst, D., Miller, B., Sweeney, C., Oltmans, S., Nance, D., Hintsa, E., Dutton, G., Watts, L. A., Spackman, R., Rosenlof, K., Ray, E., Zondlo, M., Diao, M., Mahoney, M. J., Chahine, M., Olsen, E., Keeling, R., Bent, J., Atlas, E. A., Lueb, R., Patra, P., Ishijima, K., Engelen, R., Nassar, R., Jones, D. B., Mikaloff-Fletcher, S. (2011), HIAPER Pole-to-Pole Observations (HIPPO): Fine grained, global scale measurements for determining rates for transport, surface emissions, and removal of climatically important atmospheric gases and aerosols, *Philos. T. Roy. Soc. A*, 369, 2073–2086, doi:10.1098/rsta.2010.0313, 2011.

Wunch, D., Toon, G. C., Wennberg, P. O., Wofsy, S. C., Stephens, B. B., Fischer, M. L., Uchino, O., Abshire, J. B., Bernath, P., Biraud, S. C., Blavier, J.-F. L., Boone, C., Bowman, K. P., Browell, E. V., Campos, T., Connor, B. J., Daube, B. C., Deutscher, N. M., Diao, M., Elkins, J. W., Gerbig, C., Gottlieb, E., Griffith, D. W. T., Hurst, D. F., Jimenez, R., Keppel-Aleks, G., Kort, E. A., Macatangay, R., Machida, T., Matsueda, H., Moore, F., Morino, I., Park, S., Robinson, J., Roehl, C. M., Sawa, Y., Sherlock, V., Sweeney, C., Tanaka, T., Zondlo, M. A. (2010), Calibration of the Total Carbon Column Observing Network using aircraft profile data, Atmos. Meas. Tech., 3, 1351–1362, doi:10.5194/amt-3-1351-2010, http://www.atmos-meas-tech.net/3/1351/2010/.

Wunch, D., Toon, G. C., Blavier, J.-F. L., Washenfelder, R. A., Notholt, J., Connor, B. J., Griffith, D. W. T., Sherlock, V., Wennberg, P. O. (2011a), The Total Carbon Column Observing Network, *Phil. Trans. R. Soc. A*, 369, 2087–2112, doi:10.1098/rsta.2010.0240.

Wunch, D., Wennberg, P. O., Toon, G. C. , Connor, B. J., Fisher, B., Osterman, G. B., Frankenberg, C., Mandrake, L., O'Dell, C., Ahonen, P., Biraud, S. C., Castano, R., Cressie, N., Crisp, D.,

Deutscher, N. M., Eldering, A., Fisher, M. L., Griffith, D. W. T., Gunson, M., Heikkinen, P., Keppel-Aleks, G., Kyrö, E., Lindenmaier, R., Macatangay, R., Mendonca, J., Messerschmidt, J., Miller, C. E., Morino, I., Notholt, J., Oyafuso, F. A., Rettinger, M., Robinson, J., Roehl, C. M., Salawitch, R. J., Sherlock, V., Strong, K., Sussmann, R., Tanaka, T., Thompson, D. R., Uchino, O., Warneke, T., Wofsy, S. C. (2011b), A method for evaluating bias in global measurements of CO_2 total columns from space, *Atmos. Chem. Phys.*, 11, 12317-12337.

Yoshida, Y., Ota, Y., Eguchi, N., Kikuchi, N., Nobuta, K., Tran, H., Morino, I., Yokota, T. (2011): Retrieval algorithm for CO_2 and CH_4 column abundances from short-wavelength infrared spectral observations by the Greenhouse gases observing satellite, *Atmos. Meas. Tech.*, 4, 717–734, doi:10.5194/amt-4-717-2011.

11. Tables

Table 1: GHG-CCI XCO_2 and XCH_4 random and systematic uncertainty requirements for measurements over land. Abbreviations: G=Goal requirement (the maximum that needs to be achieved; better performance likely not needed as other errors (e.g., modelling errors) will dominate), B=Breakthrough requirement ("good" performance somewhere between G and T), T=Threshold requirement (the minimum that needs to be achieved for the specified application, here: global regional-scale surface flux inverse modelling). See also main text for a detailed explanation. From GHG-CCI User Requirements Document (URD, Buchwitz et al., 2011a).

Requirements for regional CO_2 and CH_4 source/sink determination using SCIAMACHY/ENVISAT and TANSO/GOSAT					
Parameter	**Requirement type**	**Random error**		**Systematic error**	**Stability**
		Single observation	**1000^2 km^2, monthly**		
XCO_2	G	< 1 ppm	< 0.3 ppm	< 0.2 ppm (absolute)	As systematic error but per year
	B	< 3 ppm	< 1.0 ppm	< 0.3 ppm (relative)	-"-
	T	< 8 ppm	< 1.3 ppm	< 0.5 ppm (relative)	-"-
XCH_4	G	< 9 ppb	< 3 ppb	< 1 ppb (absolute)	As systematic error but per year
	B	< 17 ppb	< 5 ppb	< 5 ppb (relative)	-"-
	T	< 34 ppb	< 11 ppb	< 10 ppb (relative)	-"-

Table 2: Overview GHG-CCI ECV Core Algorithms (ECAs). Details on each of these algorithms are also given in the GHG-CCI ATBD (Reuter et al., 2012a) and in Buchwitz et al., 2012a. Column "Algorithm short name" lists the GHG-CCI algorithm identifiers (names in brackets are names (also) used in the literature (see column "References")).

GHG-CCI ECV Core Algorithms (ECAs)				
Algorithm ID	**Data product**	**Sensor**	**Algorithm short name**	**References**
CO2_SCI_WFMD	XCO_2	SCIAMACHY/ ENVISAT	WFMD (WFM-DOAS)	*Schneising et al.2011, 2012; Heymann et al., 2012b*
CO2_SCI_BESD	XCO_2	SCIAMACHY	BESD	*Reuter et al., 2010, 2011*
CO2_GOS_OCFP	XCO_2	TANSO/GOSAT	OCFP (UoL-FP)	*Cogan et al., 2012*
CO2_GOS_SRFP	XCO_2	TANSO/GOSAT	SRFP (RemoteC)	*Butz et al., 2011*
CH4_SCI_WFMD	XCH_4	SCIAMACHY	WFMD (WFM-DOAS)	*Schneising et al.,2010, 2011*
CH4_SCI_IMAP	XCH_4	SCIAMACHY	IMAP	*Frankenberg et al., 2011*
CH4_GOS_OCFP	XCH_4	TANSO/GOSAT	OCFP	*Parker et al., 2011*
CH4_GOS_OCPR	XCH_4	TANSO/GOSAT	OCPR	*Parker et al., 2011*
CH4_GOS_SRFP	XCH_4	TANSO/GOSAT	SRFP	*Butz et al., 2011*
CH4_GOS_SRPR	XCH_4	TANSO/GOSAT	SRPR	*Schepers et al., 2012*

Table 3: Overview GHG-CCI Additional Constraints Algorithms (ACAs). (*) Note that CO2_SCI_ONPD is a new algorithm "similar" as the one described in Noël et al., 2011, which has been added in the 2nd year of GHG-CCI. Details on each of these algorithms are also given in the GHG-CCI ATBD (Reuter et al., 2012a) and in Buchwitz et al., 2012a.

GHG-CCI Additional Constraints Algorithms (ACAs)				
Algorithm ID	**Data product**	**Sensor**	**Algorithm**	**References**
CO2_AIR_NLIS	Mid/upper trop. column	AIRS	NLIS	*Crevoisier et al., 2004*
CO2_IAS_NLIS	Mid/upper trop. column	IASI	NLIS	*Crevoisier et al., 2009a*
CO2_ACE_CLRS	Upper trop. / strat. profile	ACE-FTS	CLRS	*Foucher et al., 2009*
CO2_SCI_ONPD	Stratospheric profile	SCIAMACHY	ONPD	*(Noël et al., 2011)* (*)
CH4_IAS_NLIS	Upper trop. / strat. profile	IASI	NLIS	*Crevoisier et al., 2009b*
CH4_MIP_IMK	Upper trop. / strat. profile	MIPAS	KIT/IMK MIPAS	*von Clarmann et al., 2009*
CH4_SCI_ONPD	Stratospheric profile	SCIAMACHY	ONPD	*Noël et al., 2011*

1167

1168 **Table 4:** TCCON sites as used for the validation of the satellite-derived XCH_4 and XCO_2 Round

1169 Robin (RR) data products by the GHG-CCI validation team (from Notholt et al., 2012).

TCCON validation sites used for GHG-CCI Round Robin					
Name	**ID**	**Latitude [deg]**	**Longitude [deg]**	**Altitude [km]**	**Time coverage MM/YYYY-MM/YYYY**
Bialystok	BIA	53.231	23.025	0.183	03/2009 - 03/2011
Bremen	BRE	53.104	8.850	0.027	01/2009 - 12/2010
Karlsruhe	KAR	49.102	8.440	0.110	04/2010 - 05/2011
Orleans	ORL	47.965	2.113	0.132	08/2009 - 11/2010
Garmisch	GAR	47.476	11.063	0.744	05/2009 - 12/2010
ParkFalls	PAR	45.945	-90.273	0.442	06/2004 - 04/2011
Lamont	LAM	36.604	-97.486	0.320	07/2008 - 05/2011
Darwin	DAR	-12.425	130.891	0.030	08/2005 - 02/2011
Wollongong	WOL	-34.406	150.879	0.030	06/2008 - 03/2011
Lauder	LAU	-45.050	169.680	0.370	06/2004 - 06/2011

1170

1171

1172

Table 5: Estimated precision and biases of the satellite XCO_2 (top) and XCH_4 (bottom) GHG-CCI core data products retrieved with ECAs obtained from comparisons with ground-based TCCON retrievals (see Figure 3 and 4 for details). *) The exact version number for BESD is v01.00.01. Numbers in curved brackets are for SCIAMACHY methane retrievals during 2003-2005, i.e., before significant detector degradation of the methane channel: values from Buchwitz et al., 2012a, are indicated by #) and value from Schneising et al., 2012, is indicated by §). Values in square brackets for SCIAMACHY methane retrieval are from Buchwitz et al., 2012a, based on an analysis of all available retrievals (all years) and using a different assessment method. Also listed are the GHG-CCI user requirements as given the GHG-CCI User Requirements Document (URD (Buchwitz et al., 2011a), see also Table 1, e.g., for the explanation of T, B, G).

Comparison of GHG-CCI core data products (ECAs) with TCCON				
XCO_2 [ppm]				
Algorithm	**Sensor**	**Estimated precision single observation**	**Estimated relative biases**	**Number of satellite obs.**
WFMD v2.2	SCIAMACHY	5.1	1.3	30752
BESD v1 *)	SCIAMACHY	2.3	0.7	9467
OCFP v3.0	TANSO	2.7	0.6	2830
SRFP v1.1	TANSO	2.8	0.9	2558
Required (URD):		< 8(T), 3(B), 1(G)	< 0.5(T), 0.3(B), 0.2(G)	-
XCH_4 [ppb]				
Algorithm	**Sensor**	**Estimated precision single observation**	**Estimated relative biases**	**Number of satellite obs.**
WFMD v2.3	SCIAMACHY	82 (~30#))	11 (~3§)) [4-12#)]	37628
IMAP v6.0	SCIAMACHY	50 (~30#))	15 [4-13#)]	39489
OCFP v3.2	TANSO	16	8	3176
SRFP v1.1	TANSO	15	3	2558
OCPR v3.2	TANSO	13	2	7323
SRPR v1.1	TANSO	14	3	4900
Required (URD):		< 34(T), 17(B), 9(G)	< 10(T), 5(B), 3(G)	-

Table 6: Overview of the planned content of the GHG-CCI CRDP. §) see Table 2 and Table 3, *) may end later, +) may start earlier, #) mainly high latitudes. Products: (1) mid/upper tropospheric columns, (2) (primarily) stratospheric vertical profiles.

Planned content of the GHG-CCI Climate Research Data Package (CRDP)				
Data products generated with ECV Core Algorithms (ECAs)				
Product ID	**Product** (Level 2, mixing ratios)	**Algorithm** §)	**Coverage**	**Comment**
XCO2_SCIA	XCO_2	BESD	Global, land, 2003-2010*)	-
XCO2_GOSAT	XCO_2	OCFP and SRFP	Global, mid 2009-2010*)	2 alternative products
XCO2_EMMA	XCO_2	EMMA	Global, mid 2009-2010*)	Merged SCIA and GOSAT
XCH4_SCIA	XCH_4	IMAP and WFMD	Global, 2003-2010*)	2 alternative products
XCH4_GOSAT	XCH_4	SRFP and OCPR	Global, mid 2009-2010*)	2 alternative products
Data products generated with Additional Constraints Algorithms (ACAs)				
Product ID	**Product** (Level 2, mixing ratios)	**Algorithm** §)	**Coverage**	**Comment**
CO2_AIRS	CO_2 (1)	NLIS	Tropics, 2003-2007	-
CO2_IASI	CO_2 (1)	NLIS	Tropics, 2007-2010*)	-
CH4_IASI	CH_4 (1)	NLIS	Tropics, 2007-2010*)	-
CH4_SCIA_OCC	CH_4 (2)	ONPD	NH mid/high lat., 2003-2010*)	-
CO2_SCI_OCC	CO_2 (2)	ONPD	NH mid/high lat., 2003-2010*)	-
CH4_MIPAS	CH_4 (2)	KIT/IMK MIPAS	Global, 2005+)-2010*)	-
CO2_ACEFTS	CO_2 (2)	CLRS	Global#), 2004-2010*)	-

12. Figures

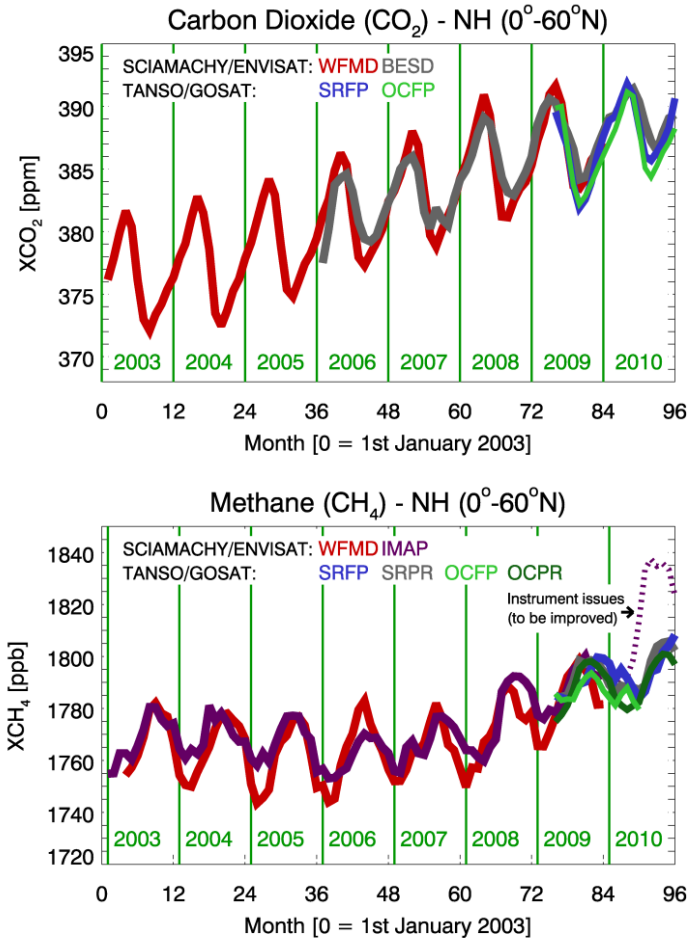

Figure 1: Top: Northern hemispheric monthly mean XCO_2 time series retrieved from SCIAMACHY/ENVISAT (algorithms: WFMD and BESD) and TANSO/GOSAT (algorithms: SRFP and OCFP) satellite data. Shown are monthly mean values for the 0°-60°N latitude range. Clearly visible is the CO_2 increase primarily caused by the burning of fossil fuels and the seasonal cycle primarily caused by uptake and release of CO_2 by the terrestrial biosphere. Bottom: As top panel but for XCH_4 (algorithms: SCIAMACHY: WFMD and IMAP, TANSO: SRFP, SRPR, OCFP, OCPR). The seasonal cycle of methane is primarily due to wetland emissions, which are largest in summer / early autumn, when soils are warm and humid. Also clearly visible is the not yet well understood recent methane increase. For a color version of this figure please have a look at the on-line version of this publication.

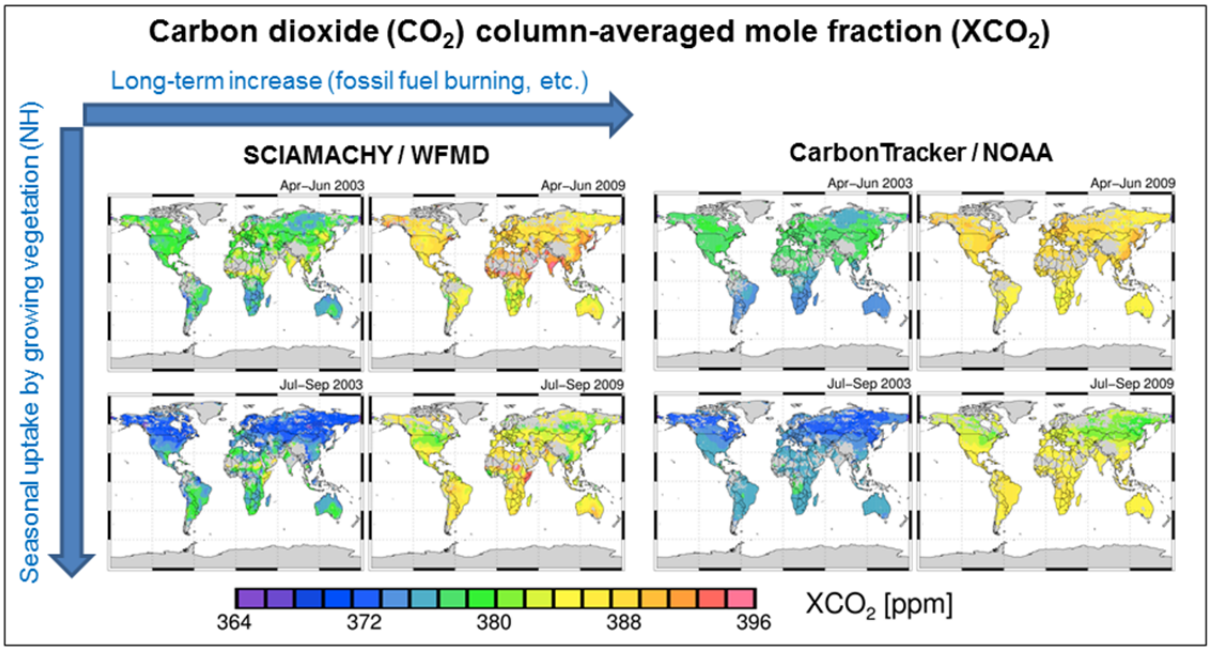

Figure 2: Global XCO_2 maps from SCIAMACHY (left) and CarbonTracker (right) for two seasons (April-June, top, and July-September, bottom) and two years (2003 and 2009). The CarbonTracker model data have been sampled according to the SCIAMACHY measurements and the SCIAMACHY averaging kernels have been applied to CarbonTracker. Figure adapted from Heymann et al., 2012b. For a color version of this figure please have a look at the on-line version of this publication.

1217

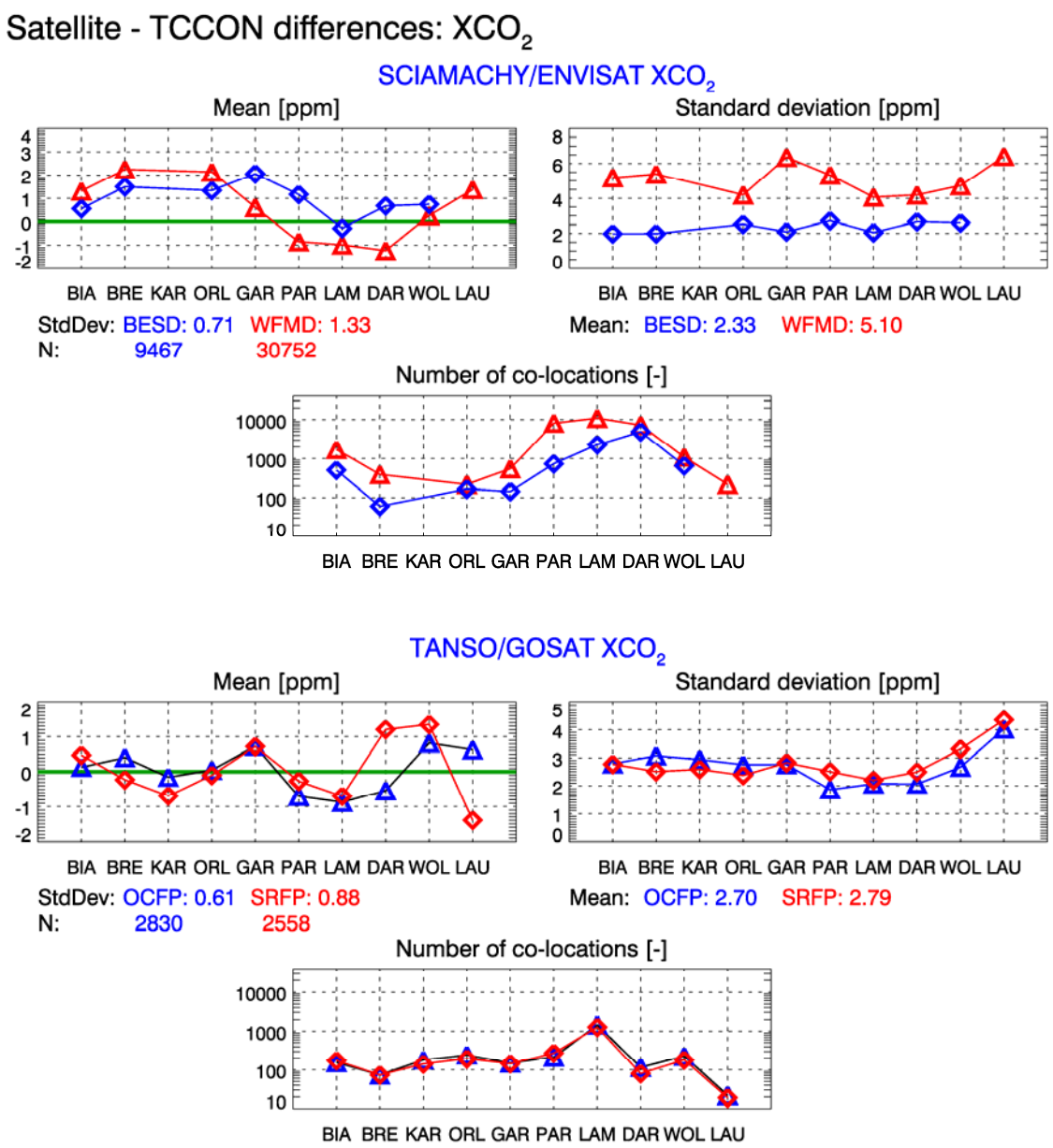

1218

1219

1220

1221 **Figure 3:** Comparison of the GHG-CCI core ECV XCO_2 data products from
1222 SCIAMACHY/ENVISAT (top half, i.e., first 3 panels) and TANSO/GOSAT (bottom half) with
1223 TCCON ground-based observations (see Table 4 for details on the TCCON sites). Shown are the mean
1224 difference ("Mean" in ppm) with respect to TCCON (left), the standard deviation of the difference
1225 (right), and the number of co-locations (middle). A 500 km / 2 hour spatio-temporal co-location
1226 criterion has been used to compute the satellite – TCCON differences. The numerical values listed are:
1227 Left: "StdDev" is the standard deviation of the mean differences as obtained at the TCCON sites, i.e.,
1228 a measure of the station-to-station bias, and can be interpreted as relative accuracy (relative bias) of
1229 the satellite retrievals. "N" is the number of satellite data used for comparison (only those data points
1230 are shown where at least 10 satellite observations are available for a given site). Right: "Mean" is the
1231 mean value of the standard deviations show by the symbols and is a measure of the achieved overall
1232 precision. Note that the number of co-locations is significantly different for the different TCCON sites,
1233 e.g., due to clouds. For a color version of this figure please have a look at the on-line version of this
1234 publication.

1235

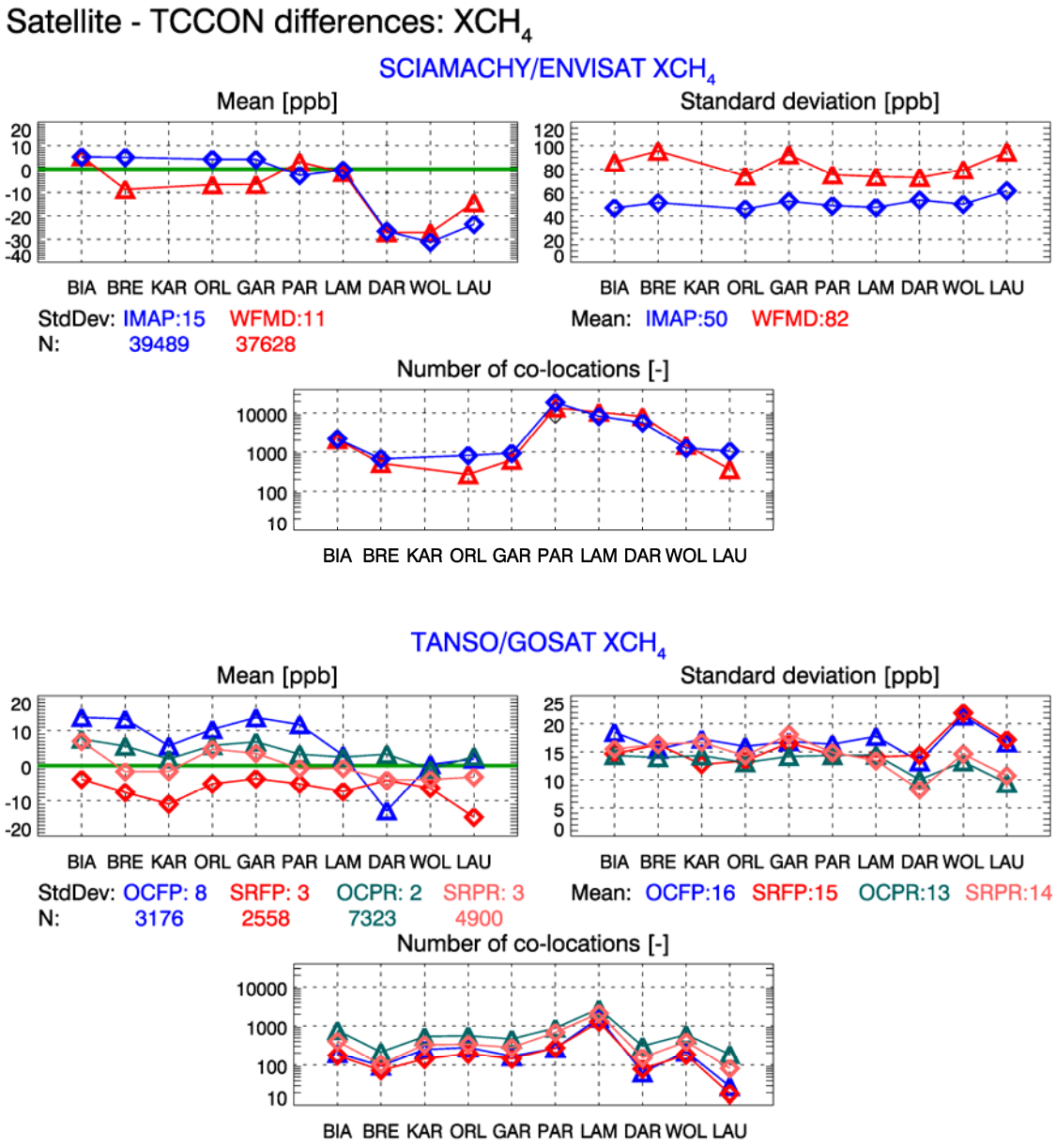

Figure 4: As Fig. 3 but for the GHG-CCI XCH_4 data products.

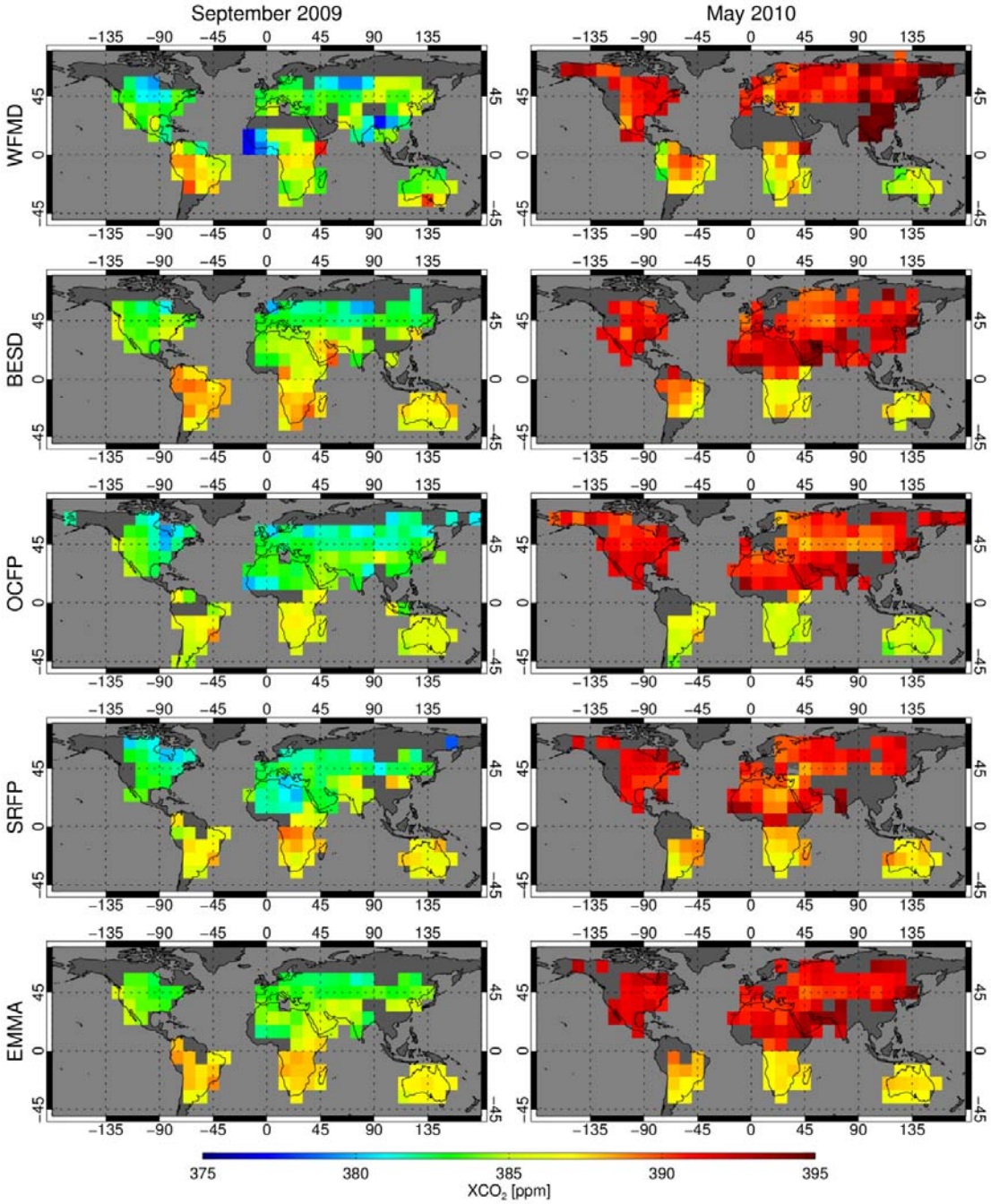

Figure 5: Maps of monthly mean XCO_2 at 10^ox10^o resolution as obtained using different GHG-CCI retrieval algorithms: WFMD and BESD for SCIAMACHY, OCFP and SRFP for TANSO and SCIAMACHY and TANSO merged using EMMA for September 2009 (left) and May 2012 (right). For a color version of this figure please have a look at the on-line version of this publication.

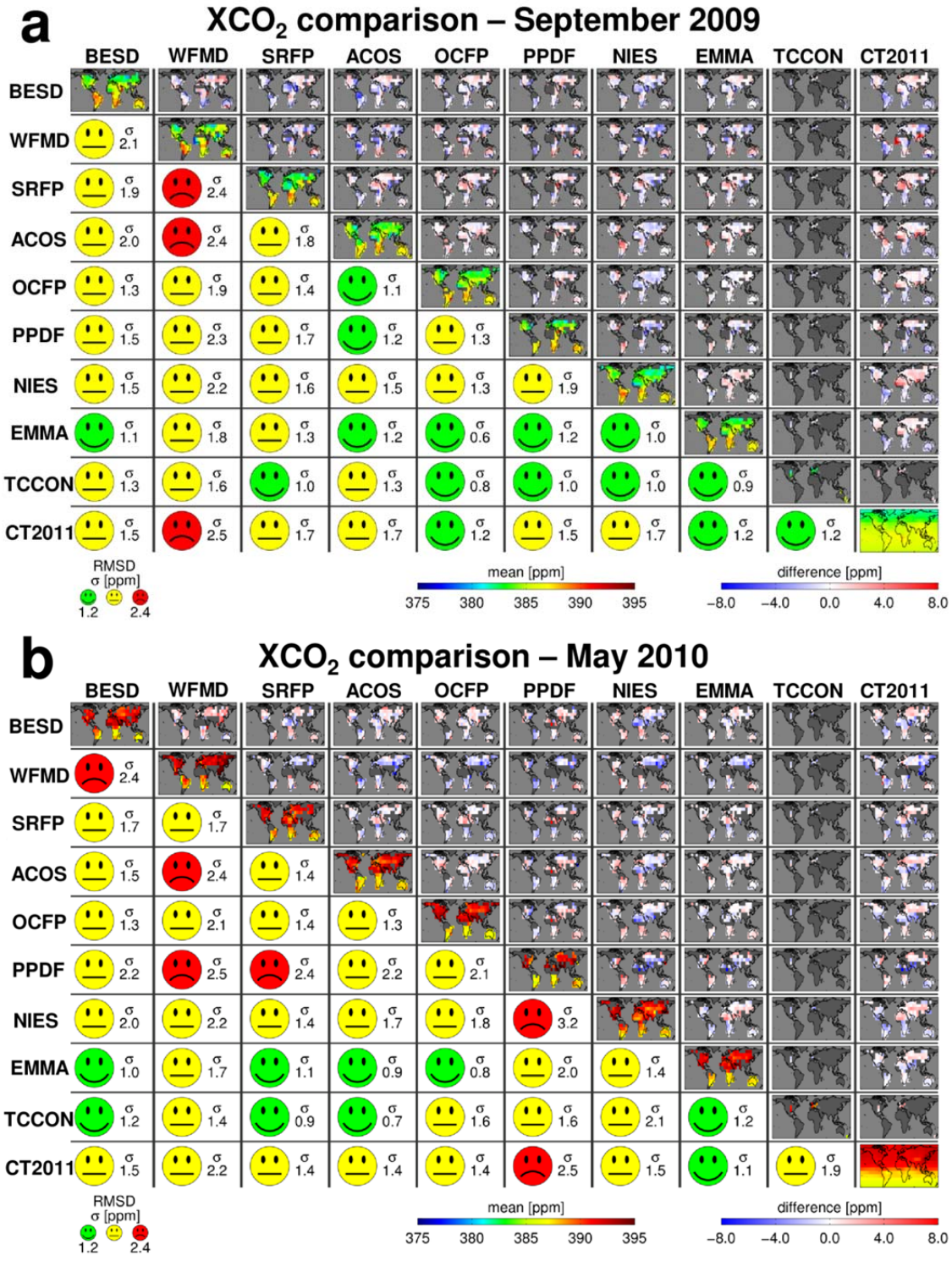
a
XCO2 comparison – September 2009
BESD
WFMD
SRFP
ACOS
OCFP
PPDF
NIES
EMMA
TCCON
CT2011
RMSD σ [ppm]
1.2
2.4
mean [ppm]
375 380 385 390 395
difference [ppm]
−8.0 −4.0 0.0 4.0 8.0
b
XCO2 comparison – May 2010
BESD
WFMD
SRFP
ACOS
OCFP
PPDF
NIES
EMMA
TCCON
CT2011
RMSD σ [ppm]
1.2
2.4
mean [ppm]
375 380 385 390 395
difference [ppm]
−8.0 −4.0 0.0 4.0 8.0

1253

1254 **Figure 6:** Comparison matrix of monthly XCO_2 maps for September 2009 (top (a)) and May 2010
1255 (bottom (b)) generated using several individual satellite retrieval algorithms: BESD and WFMD for
1256 SCIAMACHY and SRFP, ACOS, OCFP, PPDF, NIES for TANSO. The EMMA data product has
1257 been generated from the ensemble of the individual SCIAMACHY and TANSO XCO_2 data products
1258 (see main text for details). Also shown is XCO_2 from TCCON and NOAA's CarbonTracker (CT,
1259 v2011). The diagonal elements show the monthly XCO_2 maps (using color bar "mean"). The above
1260 diagonal elements show the XCO_2 differences for all combinations (color bar "difference"). The below
1261 diagonal elements show the numerical values of the Root Mean Square Difference (RMSD) as well as
1262 color coded smileys of the RMSD (green: RMSD < 1.2 ppm, red: RMSD > 2.4 ppm, otherwise
1263 yellow). For a color version of this figure please have a look at the on-line version of this publication.

1264

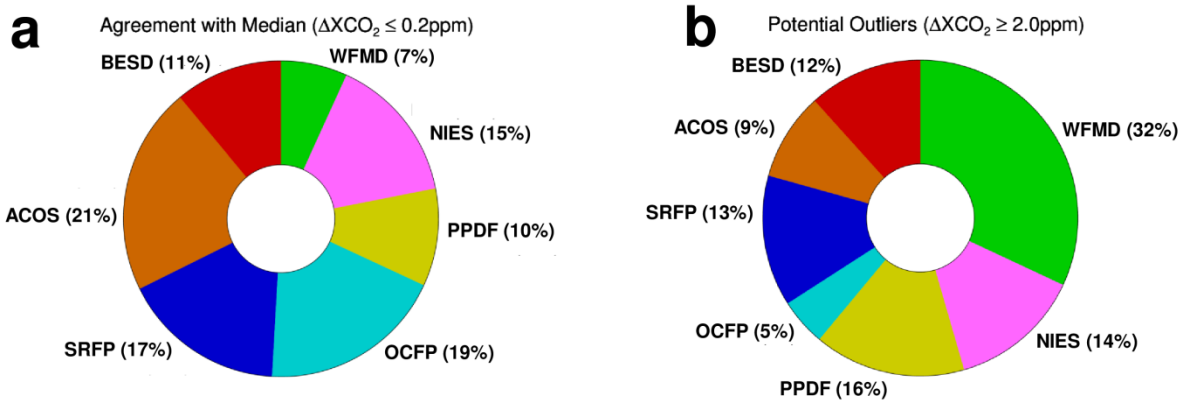

Figure 7: Pie charts showing the agreement (left) and disagreement (right) with the EMMA median obtained using the listed satellite XCO_2 data products. The figure has been obtained using the EMMA Level 3 data product (10^ox10^o, monthly = 1 voxel). For each voxel the mean XCO_2 value for each algorithm has been computed and the median using all algorithms. The "Agreement with the Median" (left) has been computed as follows: For algorithm *i* the number of voxels which agree with the median within 0.2 ppm have been counted (= N_i). 100% corresponds to the sum of these numbers ($N = \Sigma_i N_i$). The percentages shown are N_i/N*100%. The percentages of "Potential Outliers" (right) have been calculated using the same method except that all voxels have been counted where the differences to the median are larger than 2 ppm. As can be seen from the left figure, the data product which agrees best with the median is the ACOS product (v2.9, 21% agreement) followed by the similar OCFP algorithm (19% agreement). The largest number of potential outliers have the data products generated with the two very fast algorithms WFMD (32%) and PPDF (16%). For a color version of this figure please have a look at the on-line version of this publication.

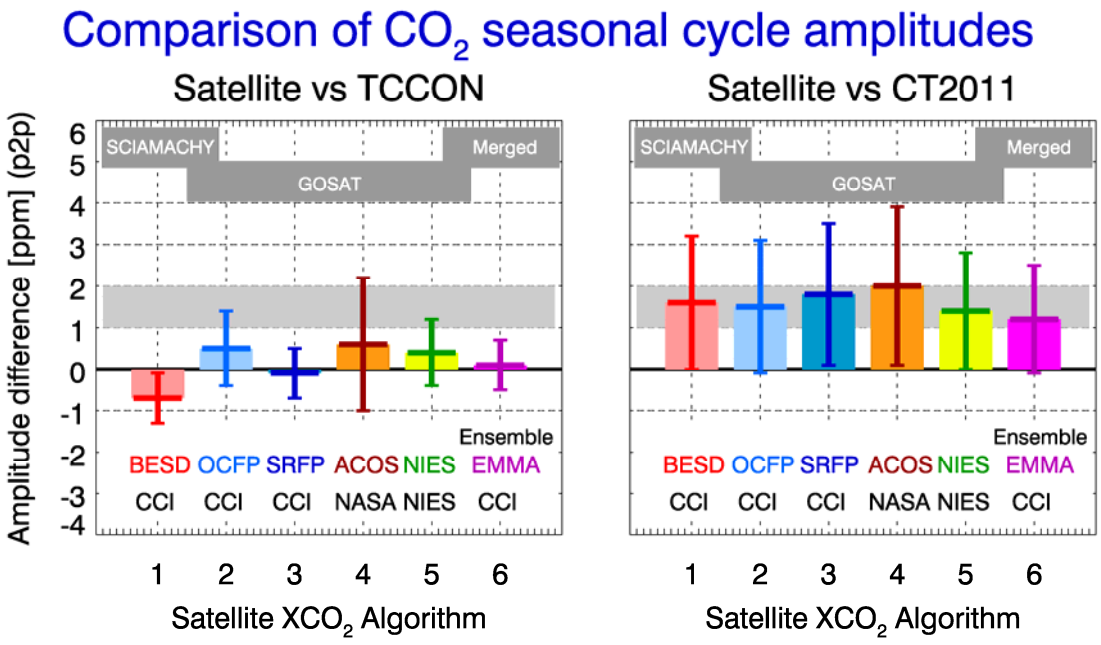

Figure 8: Comparison of the XCO_2 seasonal cycle amplitude (peak-to-peak) of the individual XCO_2 algorithms and EMMA with TCCON (left) and CarbonTracker (v2011) (right). The figure has been adapted from Reuter et al., 2013, where results for all investigated XCO_2 data products are shown, i.e., including WFMD and PPDF, not shown here as their error bars do not indicate good enough agreement with TCCON. As can be seen, all XCO_2 satellite data suggest that the amplitude of the CO_2 seasonal cycle is underestimated by CarbonTracker by approximately 1.5+/-0.5 ppm peak-to-peak. For a color version of this figure please have a look at the on-line version of this publication.

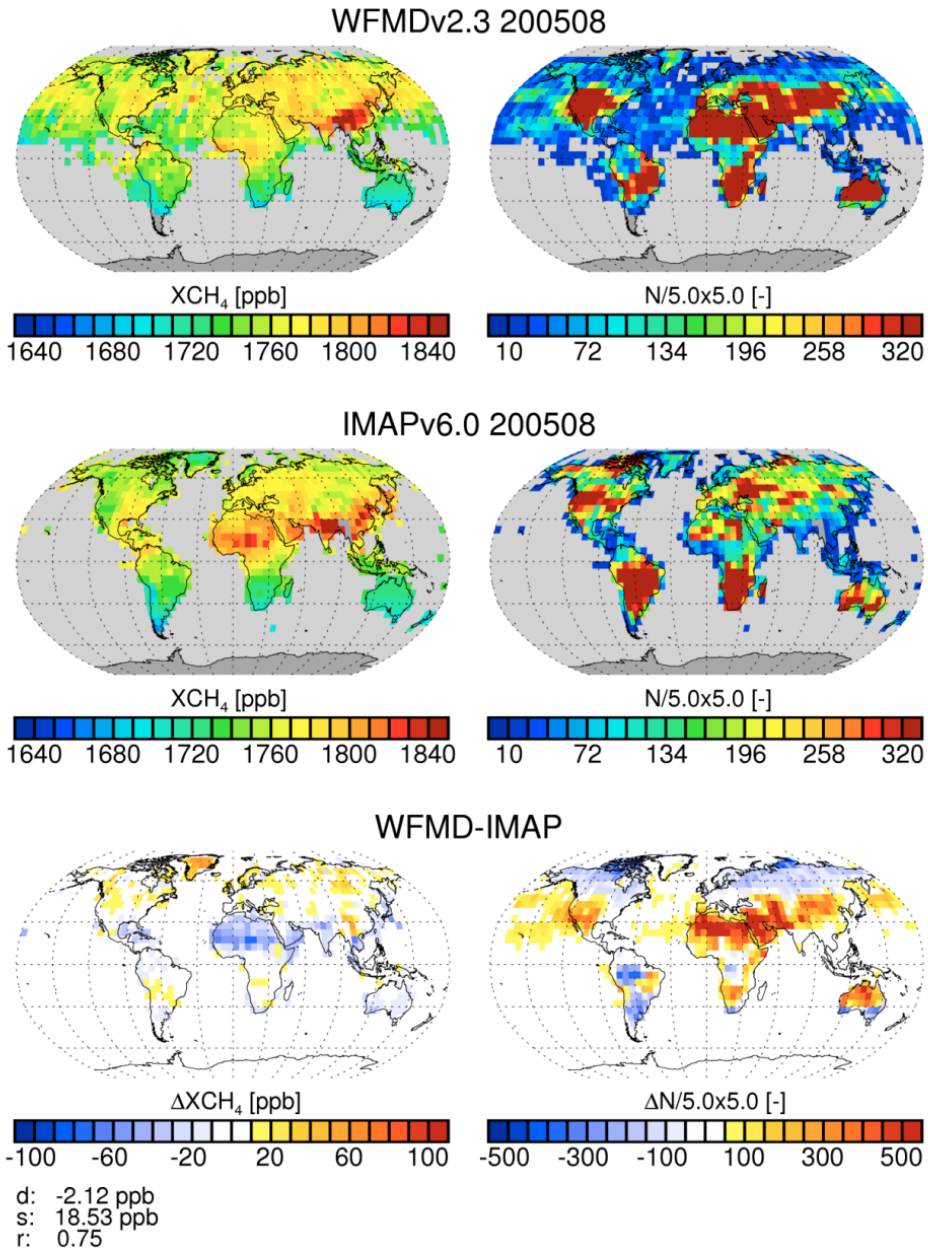

Figure 9: Comparison of two SCIAMACHY XCH_4 data products retrieved using WFMD (top) and IMAP (middle) for August 2005. Global maps of the retrieved XCH_4 are shown on the left and the number of retrievals per 5^ox5^o grid cell on the right. The WFMD-IMAP difference is shown in the bottom row. Listed in the bottom left are the following parameters: d: mean difference (-2.12 ppb), s: standard deviation of the difference (18.53 ppb), r: linear correlation coefficient (0.75). For a color version of this figure please have a look at the on-line version of this publication.

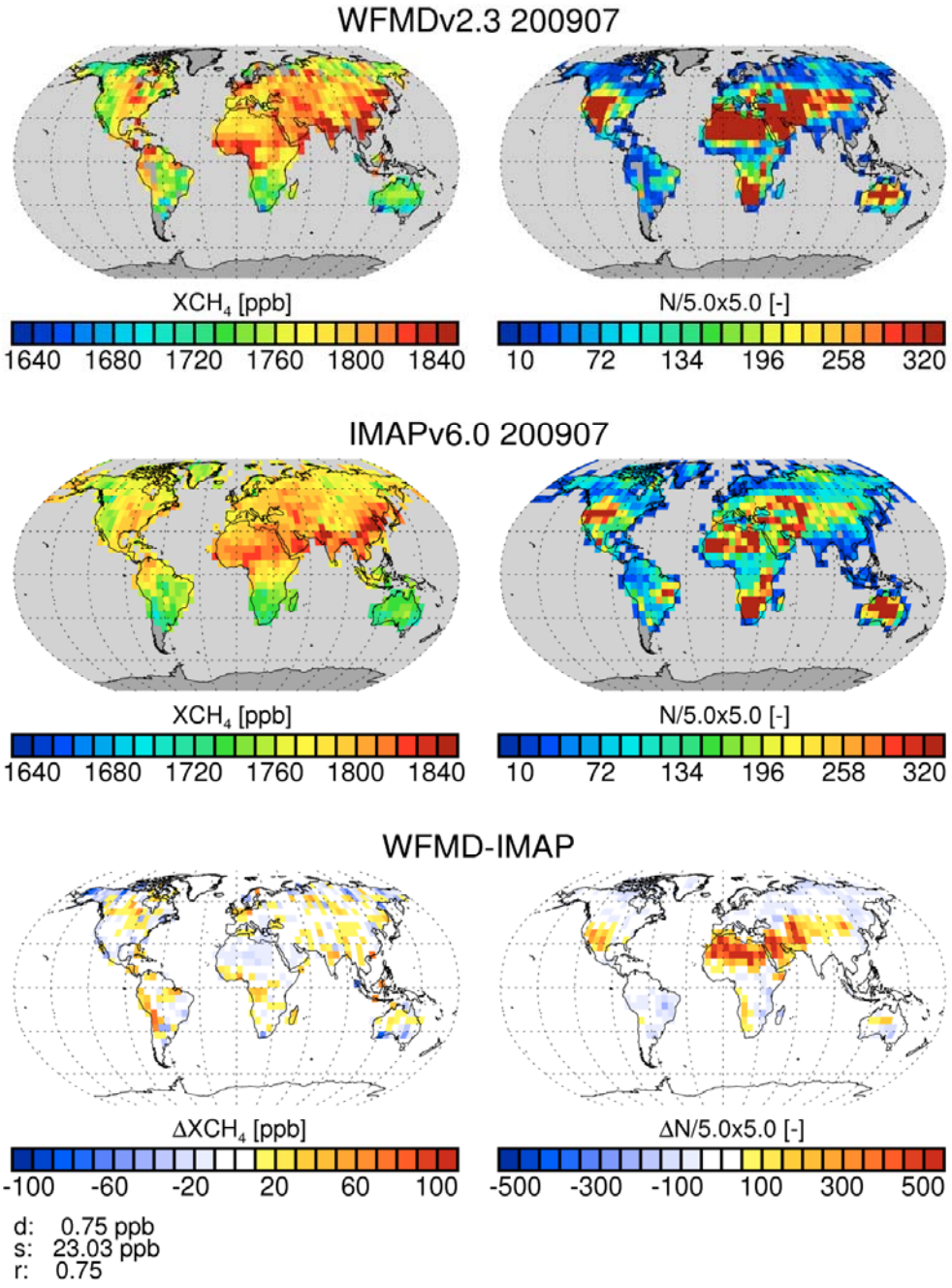

Figure 10: As Fig. 9 but for July 2009.

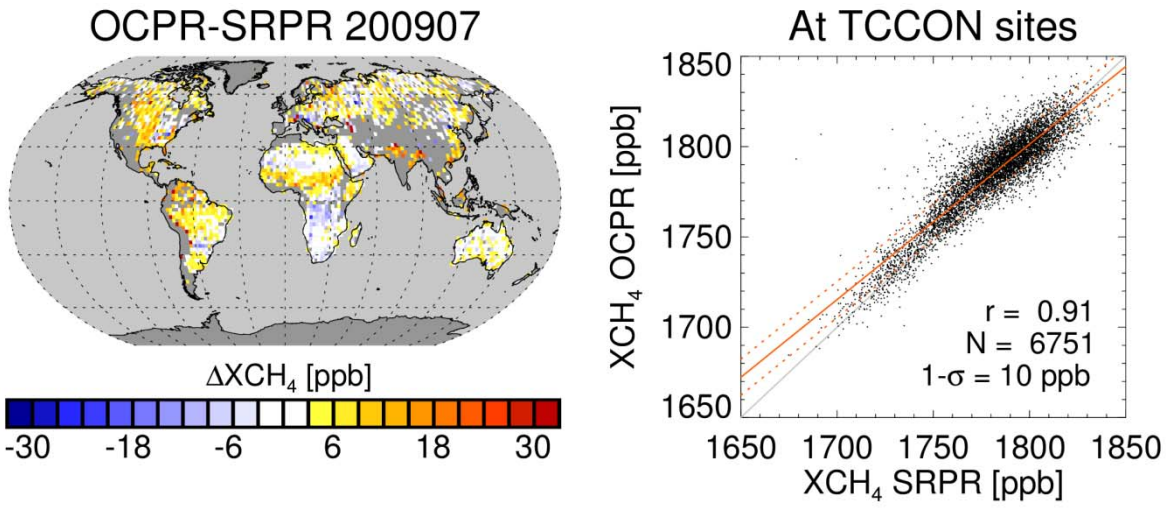

Figure 11: Comparison of the two GHG-CCI TANSO XCH_4 PR data products retrieved using the OCPR and SRPR retrieval algorithms. Left: Percentage XCH_4 difference OCPR-SRPR for July 2009. Right: Scatter plot of 6751 co-located OCPR versus SRPR retrievals at TCCON sites. The standard deviation of the difference is 10 ppb (1-sigma) and the linear correlation coefficient is 0.91. For a color version of this figure please have a look at the on-line version of this publication.